COORDINATION CHEMISTY OF CROWN THIOETHERS

WEIMIN LIANG

COORDINATION CHEMISTRY OF CROWN THIOETHERS

by

Weimin Liang©

A thesis submitted to the
School of Graduate Studies
in partial fulfilment of the
requirements for the degree of
Master of Science

Department of Chemistry
Memorial University of Newfoundland

August 1994

St. John's Newfoundland

ISBN 0-612-01882-2

ABSTRACT

This thesis describes the properties of thio-oxa crown ligands and their coordination chemistry. Chapter I briefly reviews the synthesis, conformation and coordination chemistry of crown thioethers. In Chapter II, synthesis and characterization of 1-oxa-4,7-dithiacyclononane ([9]aneOS$_2$) and 1,10-dioxa-4,7,13,16-tetrathiacyclooctadecane ([18]aneO$_2$S$_4$) are reported. Molecular mechanics calculations are reported on [9]aneOS$_2$ and the molecular structure of [18]aneO$_2$S$_4$ has been determined by X-ray methods. In Chapter III, synthesis and properties of [Pd([9]aneOS$_2$)Cl$_2$] and [Pt([9]aneOS$_2$)Cl$_2$] have been described. Variable-temperature ^{1}H and ^{13}C NMR studies reveal the unusual stereochemical non-rigidity in [Pd([9]aneOS$_2$)Cl$_2$], and the mechanism has been proposed. In Chapter IV and V, the structures of [Cu([9]aneOS$_2$)$_2$][ClO$_4$]CH$_3$CN and [Cu([9]aneOS$_2$)Br]$_2$ are presented together with their electrochemical properties. The results indicate that ligand [9]aneOS$_2$ considerably stabilizes Cu(I) over Cu(II). The synthesis and structure of [Ag([18]aneO$_2$S$_4$)]ClO$_4$ are reported in Chapter VI.

Acknowledgement

I would like to express my sincere gratitude to Dr. C.R. Lucas for his supervision of the work described in this thesis, and for his continued encouragement and helpful discussions.

I am also grateful to Dr. J.N. Bridson for X-ray crystallography and to Dr. L.K. Thompson and his group for their help with electrochemistry and magnetic studies; to Dr. C.R. Jablonski and his group for their help with nmr spectrometry; to Dr. T.B. Grindley in Dalhousie University for his help with molecular mechanics calculations on [9]aneOS_2 and to all friends of mine who have helped me thoughout my research.

Table of Contents

List of Tables

List of Figures

List of Abbreviations

DMF: N,N-dimethylformamide

DMSO: dimethylsulfoxide

SCE: aqueous saturated calomel electrode

$E_{1/2}$: half potential, $E_{1/2} = (E_{cp} + E_{ap})/2$

E^0: standard potential

[n]aneS_m (nSm): n, the number of atoms in the macrocycle; m, the number of sulfur atoms in the macrocycle

[9]aneOS_2: 1-oxa-4,7-dithiacyclononane

[18]aneO_2S_4: 1,10-dioxa-4,7,13,16-tetrathiacyclooctadecane

ECEC: E represent an electron trasfer process, and C means a chemical reaction following it.

I. Introduction

1.1. Overview of Crown Thioether Chemistry

1.1.1. Development

The era of crown thioether chemistry started over 100 years ago when Mansfeld first reported the synthesis of 1,4,7-trithiacyclononane (9S3) **1** by the reaction of ethylene bromide with sodium sulfide [1]. In 1920 Ray also reported the preparation of 9S3 by the reaction of ethylene bromide and potassium hydrosulfide [2-4]. However, both works were questioned by Bennett and coworkers [5,6]. They used mixed melting point and cryoscopic molecular weight determination to prove that Mansfeld and Ray's products were not 9S3.

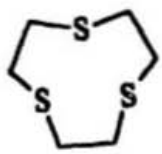

1

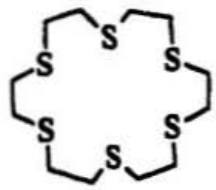

2

In 1934 Meadow and Reid [7] found that reaction of sodium ethanedithiolate with ethylene bromide gives a rubbery malodorous polymer along with a small amount of cyclic compound 1,4,7,10,13,16-hexathiacyclooctadecane (18S6) **2** in

1.7% yield. They expected to obtain 9S3 but rather they obtained 18S6 **2**. They also prepared 7,16-dioxa-1,4,10,13-tetrathiacyclooctadecane **3** from the corresponding dimercaptan and dihalide. Coming more than 30 years before the milestone discovery of the oxygen-containing crown ethers like **4** by Pederson [8], 18S6 and its potential ligating properties remained unexploited until the work of Black and McLean [9,10] in 1969. Nevertheless, from this inauspicious beginning 60 years ago the chemistry of crown thioethers has undergone explosive development, especially during the last decade.

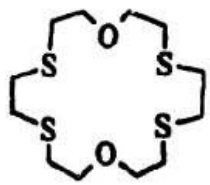

3

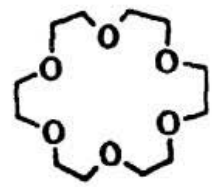

4

Comparison of thioethers to phosphines suggests that they might have extensive coordination chemistry. In principle, thioethers can act as both σ-donors and π-acceptors. The moderate π-acidity of thioethers (intermediate between that of amines and phosphines) might stabilize low oxidation states of metal ions more than amines, but less than phosphines to yield complexes with unusual reactivity [11].

The volume of work reported for thioether complexes is small compared to that for amines and phosphines. This

reflects the fact that simple thioethers (e,g. Me_2S) bind metals weakly. Their relatively low σ-donor and π-acceptor abilities [12] (compared to those of phosphines, for example), combined with steric encumbrance of the alkyl group, make simple thioethers fairly poor ligands.

The current renaissance of thioether coordination chemistry has been primarily due to the observation that crown thioethers can bind to a range of transition metal ions to form stable metal complexes [11,13-15]. The use of crown thioether ligands to stabilize and study metal-SR_2 bonding is linked to the thermodynamic macrocyclic effect in which macrocyclic complexes are often, but not always [16], observed to be of greater stability than the corresponding linear multidentate thioethers [11,17]. By enforcing coordination of binding donor groups, the crown thioether approach encourages attempts to capture metal ions in a "molecular Dewar" to generate a series of crown thioether complexes incorporating unusual stereochemistries and oxidation states [11].

The aim of this chapter is to describe recent progress in coordination chemistry of crown thioethers, with a view to likely future development and uses. The focus is on the syntheses, conformational analysis and coordination chemistry of 9S3 **1** and 18S6 **2**.

1.1.2. Research Motivation

Several facts have contributed to the rapid growth of coordination chemistry of crown thioethers over the last decade. First, the impetus stems from the role of thioether binding in biological systems such as d-biotin (involving tetrahydrothiophene) [18,19] and blue copper proteins such as plastocyanin and azurin (involving methionine) [20,21].

Research on the blue copper proteins revealed unusual optical, redox, and EPR properties that were suspected of arising from interaction of the copper ion with a thioether group from methionine [22]. The study of the binding of Cu(II) and Cu(I) centres to crown thioethers has led to a greater understanding of Cu-S interactions and the stereochemical preferences of these metal centres [85,86]. The biological activity of blue copper proteins was linked to model systems in which the coordination geometry about Cu(II) is strained [in an entatic state] [23,24] such that the Cu^{2+}/Cu^{+} couple occurs at a particularly positive potential, which indicates the Cu(I) is stabilized. The ability of crown thioethers to modify the electronic structure of coordination metal centres is inherent in this approach.

The other stimulus concerns the possible analogy between thioethers and phosphines, which suggests that thioethers might have extensive and industrially useful coordination

chemistry. This possibility spurred the earlier efforts to examine the complexes of macrocyclic thioethers [25,26].

Despite these interests in crown thioethers, arduous synthetic routes to the ligands severely impeded extensive investigation of their chemistry. This is particularly true of 9S3, the first synthesis of which proceeded in such low yield (0.04%) [27] as to preclude further study. However, advances in synthetic methodology in the last ten years opened the door to work on the coordination chemistry of crown thioethers. Since the cesium salt method was introduced in the cyclization reactions [28,29], these formerly rare and precious ligands are now readily available.

Developments in both organometallic and bioinorganic chemistry focus on the reactivity of metal complexes. This arises in two contexts: (i) practical industrial applications and (ii) fundamental comprehension of how metalloenzymes and metal-containing redox proteins function. Such interest naturally spurs attempts to control the reactivity of metal ions. Experimentally accessible parameters include coordination numbers, stereochemistry, redox potential, and steric accessibility of the metal ion. The properties of metal ions may, in principle, be manipulated by ligand design [14,15].

Complexes of crown thioethers are usually considerably more stable than those comparable acyclic ligands. For this

reason, the growing attention given to crown thioethers has spurred a blossoming of thioether coordination chemistry in general. These macrocyclic ligands thereby provide entry into new chemistry, since corresponding complexes of simple thioethers often defy synthesis [30]. The development of crown thioether ligands, such as the excellent ligand 9S3, also encourages the use of them as coligands in, for example, catalytic applications and cluster chemistry [15].

In addition, macrocyclic ligands can also alter the properties of a metal ion by constricting or dilating its coordination sphere (the macrocyclic constriction effect [31-33]). Both through imposition of those unusual environments comprising predominantly or exclusively thioether coordination and through manipulation of that environment, coordination complexes of thioethers often exhibit unusual properties and reactivities. Crown thioether complexes are ideal systems in which to study the effect on optical and redox properties of geometric deformations of the coordination sphere [11,15].

With the current renaissance of thioether coordination chemistry, crown thioethers, especially 9S3, are now taking their place in the repertoire of progress in inorganic chemistry. In contrast to thioethers, phosphines presently constitute a ligand class of central importance in the chemistry of low-valent transition metals, which in turn have found extensive application in homogeneous catalysis. In some

respects the coordination chemistry of thioethers is now in a similar state of development to that of phosphines before their importance came to be appreciated some 35 years ago.

1.1.3. Applications

The ability of crown thioethers to form stable transition metal complexes indicates that they may have new applications in medicine. Radiopharmaceuticals containing ^{99m}Tc are widely used in diagnostic studies [34] and ^{99m}Tc-based imaging plays a central role in nuclear medicine [35,36]. Myocardial imaging in particular requires complexes of low charge [37]. Because crown thioethers stabilize low oxidation states, typically to produce M^{2+} and M^{+} complexes, and are often chemically robust, they have evident application to ^{99m}Tc imaging. Recently reported $[Tc(9S3)_2]^{2+}$ illustrates the possibility of controlling ^{99m}Tc biodistribution through redox tuning mediated by 9S3 and analogous crown thioethers [38]. In addition, the affinity of crown thioethers for heavy metals, and their disinterest in the biologically important ions such as Na^{+}, Ca^{2+}, and Mg^{2+}, suits crown thioethers particularly well for sequestering and elimination of toxic ions from living organisms.

Crown thioethers present obvious opportunities as the basis for the extraction of metal ions. The use of crown

thioethers for extraction of Ag^{+}, Cu^{2+}, and Hg^{2+} has been reported [39-41]. Bolkhuis and coworkers synthesized the functionalized crown thioether 5 [42], which is moderately soluble in water whereas its analog 6 is insoluble. This property could be of practical importance in the extraction of heavy metal ions from aqueous solutions.

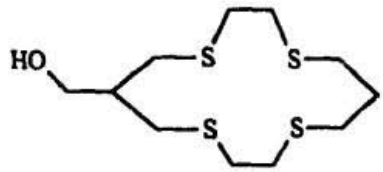

5

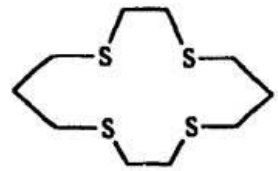

6

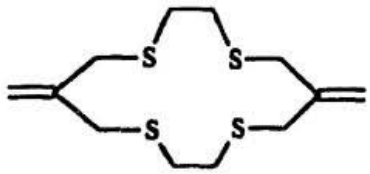

7

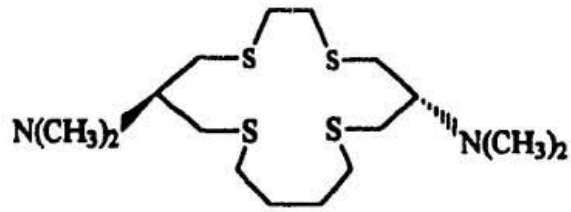

8

The synthesis of 5 involved the reaction of 7 with BH_3 to produce a very stable complex with two types of bonding, namely a Lewis interaction, $R_2S^{\cdot}$-BH_3^{-}, and covalent addition to the double bond. The Lewis interaction protects the sulfide in the subsequent oxidation step with hydrogen peroxide, which results in the formation of 5 without any oxidation of sulfide [42]. This reaction has been applied quite broadly to

functionalize double bonds by use of borane chemistry without destruction of the sulfide linkages [43].

Despite early interest in the use of thioether-based systems for catalytic hydrogenation of olefins [25,26], relatively little recent work has been devoted to this industrial application. The thioether-based catalytic system clearly deserves more attention, since crown thioethers represent an especially attractive means of imposing and controlling coordination spheres. The catalytic potential of macrocyclic thioethers was explored by Kellogg and coworkers [43-46]. They applied a Ni(0) complex of the chiral crown thioether **8** as a catalyst to the cross-coupling Grignard reaction.

Tetrathiafulvalene (TTF) **9** and its derivatives have attracted great attention lately [47]. Since the discovery of the first "organic metal" TTF-TCNQ (TCNQ = tetracyanoquinodimethane) [48], many TTF derivatives with charge-transfer properties have been reported [49,50]. Recent studies found that the redox properties of TTF change a great deal if TTF is incorporated into a crown thioether system, such as **10** [51]. Sugawara reported a complex of **11** with 2,3-dichloro-5,6-dicyano-*p*-benzoquinone showing semiconducting properties [52]. Those macrocyclic TTF-based systems present interesting physical properties and have been investigated recently with the aim of making molecular devices, sensors and

switches [47].

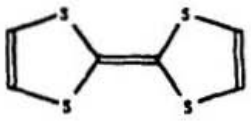

9

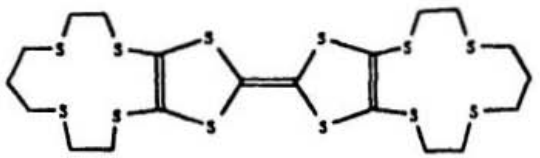

10

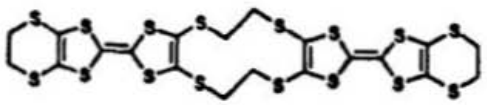

11

1.2. Syntheses of Crown Thioethers

1.2.1. Preparation of Starting materials

Syntheses of crown thioethers require the use of dithiol or α,ω-dithiolpolysulfides. Most of the simple dithioles and oligoethylene α,ω-dithiolpolysulfides used for the syntheses of macrocyclic thioethers are commercially available now. Herein are presented some of the methods that have been used to prepare these important building blocks when they are not commercially available.

Dithiols can be used to synthesize α,ω-dithiolpolysulfides. One of the experimentally simple methods to prepare thiols is the use of thiourea, as shown in scheme

1-1. The reaction involves halides and thiourea to give an iso-thiuronium salt, and hydrolysis of the latter. Earlier procedures included the use of a high boiling solvent (e.g.,triethylene glycol) to prepare the iso-thiuronium salt and to decompose it with a high boiling amine (e.g. tetraethylene pentamine) [54]. Later improvement used alkaline hydrolysis to give good yields (55-62%) of α,ω-dithiols [54].

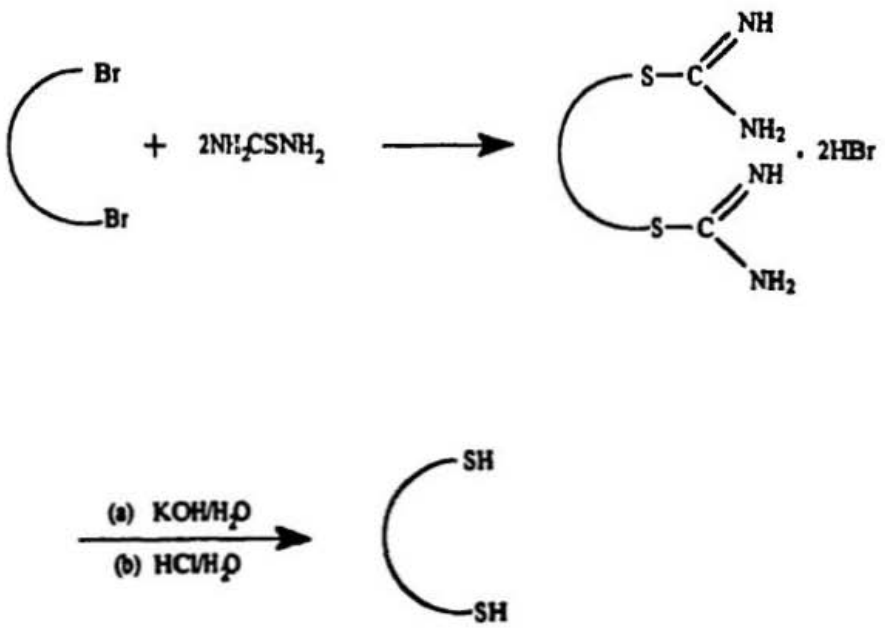

Scheme 1-1

Another direct approach to prepare dithols was reported by Martin and Greco [55]. They allowed alkyl halides to react with sodium trithiocarbonate, which is generated from sodium sulfide and carbon disulfide, and then hydrolyzed the

trithiocarbonate intermediate with acid, as shown in scheme 1-2. A good yield of dithiols (>61%) was obtained by this method [55].

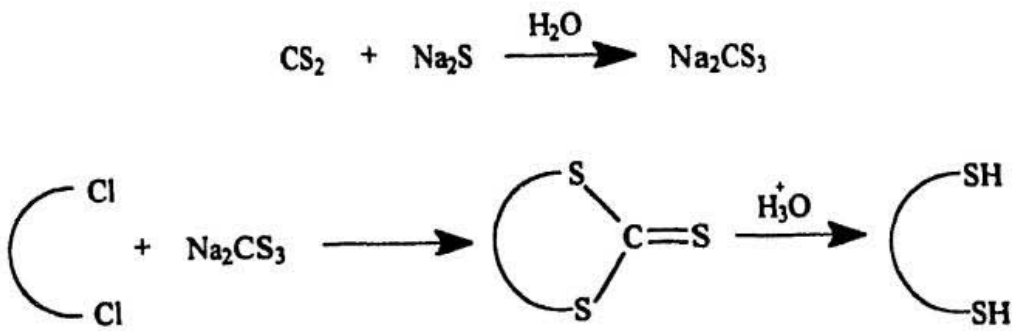

Scheme 1-2

Partyka prepared pyridine-2,6-dimethanethiol from alcohols [56]. In this method pyridine-2,6-dimethanol was refluxed with thiourea and 48% HBr solution, and then aqueous

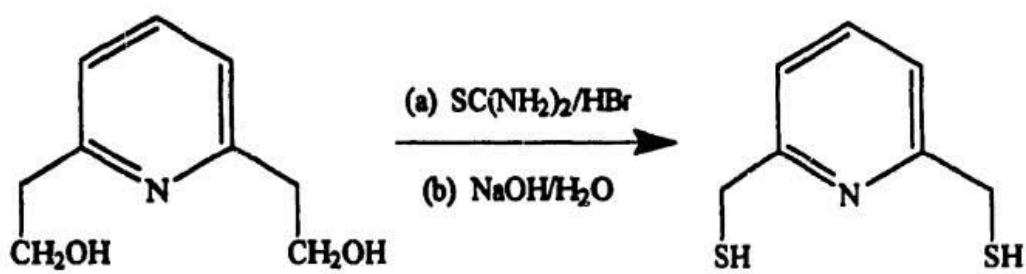

Scheme 1-3

NaOH solution was added for hydrolysis, as shown in scheme 1-3. This reaction gave a high yield (88%) of pyridine-2,6-dimethanethiol.

Polysulfides with terminal thiols are important starting materials for crown thioethers. The most common method of preparing these compounds from readily available thiols was reported by Buter and Kellogg [57]. 1,3-propanedithiol was reacted with 2-chloroethanol in absolute ethanol in the presence of sodium ethanoate to give 3,7-dithianonane-1,9-diol, which was converted to desired product via the thiourea reaction (scheme 1-4).

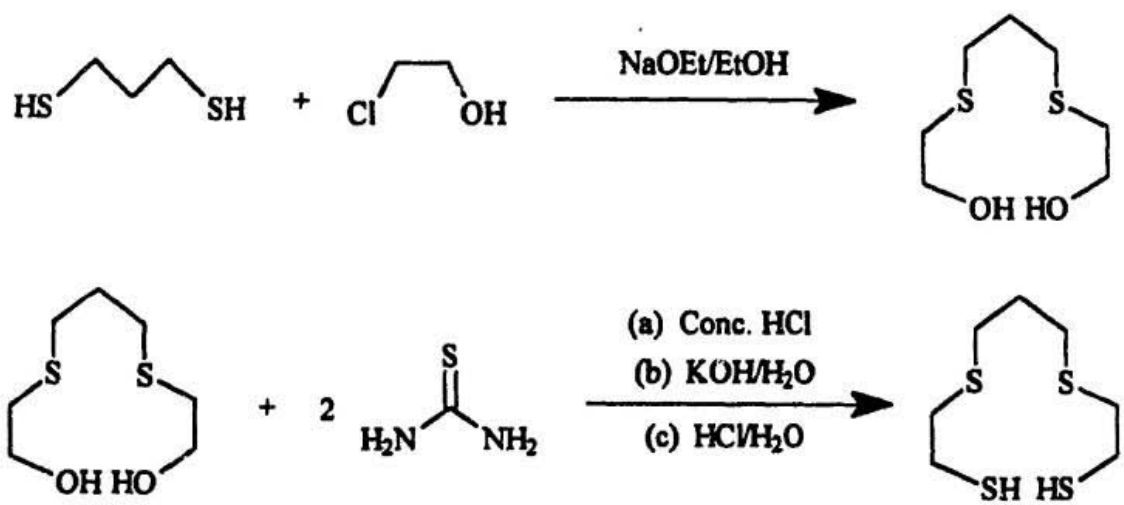

Scheme 1-4

1.2.2. General Synthetic Methods

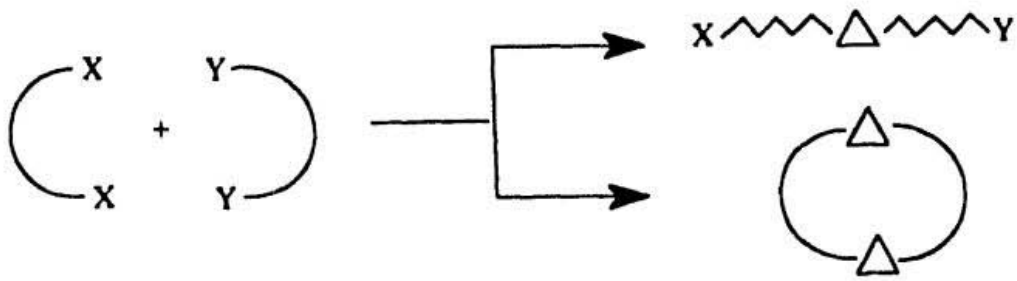

Scheme 1-5

It is important in the cyclization process to maximize the yield of desired macrocycle by choosing synthetic strategies that inhibit the competing linear polymerization reaction, as illustrated in scheme 1-5. Since the reactants for both cyclization and linear polymer compounds are the same, special conditions must be employed to avoid polymerization. The polymerization process is favoured in reactions carried out with the substrates in concentrated form or without solvent. The 1+1 or 2+2 cyclization reactions are usually slow and are favoured at low temperatures in dilute solutions and by using templates as catalysts. Polymerization can be prevented if cyclization is carried out at concentrations not exceeding 10^{-3} mol/L [58]. Therefore, in order to maximize the cyclization yield, high dilution conditions with template cations are usually used.

1.2.2.1. 1+1 Cyclization Reactions

The most used method for the preparation of crown thioethers is through the formation of two bonds, e.g. 1+1 cyclization (scheme 1-6). With the aid of the template effect of metal ions, this 1+1 cyclization process often gives high yields.

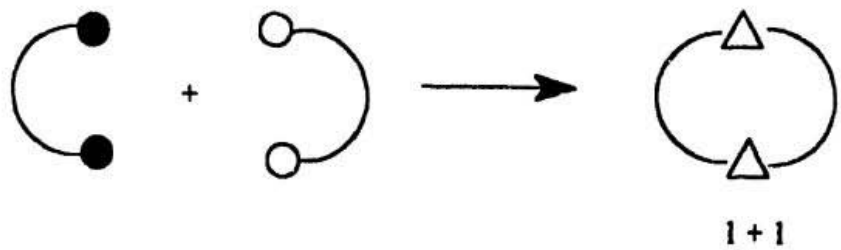

Scheme 1-6

An early attempt to synthesize 9S3 using the reaction of the disodium salt of 3-thiapentane-1,5-dithiolate with 1,2-dichloroethane gave an isolated yield of 9S3 of only 0.04% [27]. The use of cesium carbonate in the cyclization reaction, an innovation introduced by Kellogg and coworkers [28,29], has revolutionized the synthesis of 9S3. Slow addition of 3-thiapentane-1,5-dithiol and 1,2-dichloroethane to a suspension of cesium carbonate in dimethylformamide [DMF] gives 9S3 in 50% yield [59] (scheme 1-7).

Similar improvements have taken place in the synthesis of 18S6. Meadow and Reid prepared 18S6 originally in a very low

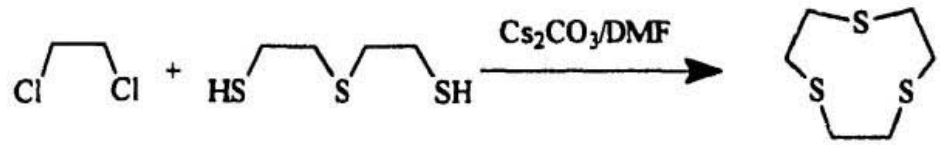

Scheme 1-7

yield of 1.7% [7]. the application of the Cs_2CO_3/DMF cyclization method, however, gave a yield of 72% on a large-scale [60] (scheme 1-8).

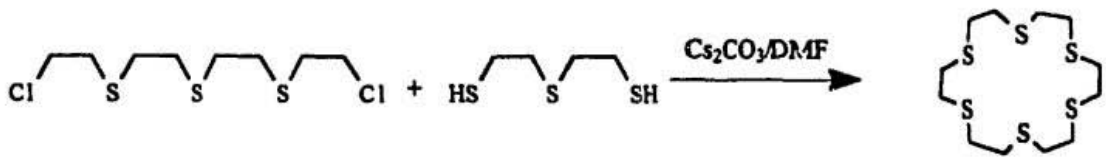

Scheme 1-8

This method was also extended to synthesize thiaaza macrocycles. With the internal amine nitrogen protected by a tosyl group, McAuley and Subramanian obtained the 1+1 cyclization product in good yield (59%) [61], as shown in scheme 1-9.

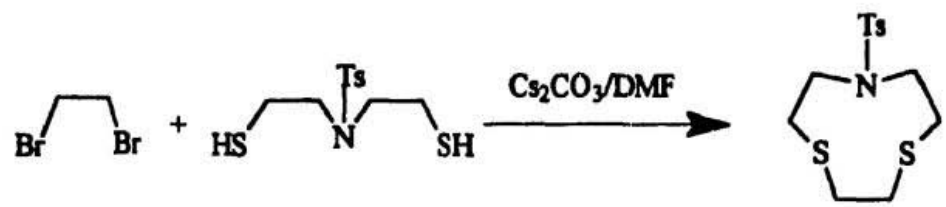

Scheme 1-9

1.2.2.2. 2+2 Cyclization Reactions

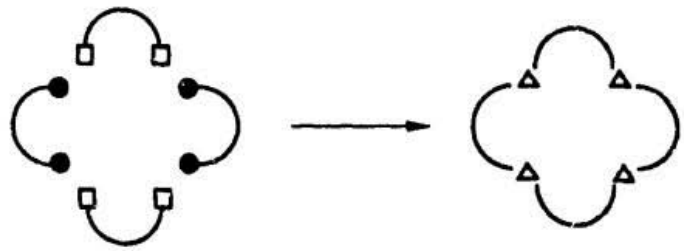

Scheme 1-10

The 2+2 cyclization process takes place between four substrate molecules, as shown in scheme 1-10. The reaction can be carried out under high-dilution conditions or with metal ions as templates. Since high-dilution conditions also give 1+1 cyclization products, these two types of cyclizations often happen in the same reaction system. A higher concentration favours the formation of 2+2 cyclization products, but also more polymer is formed [62].

Schröder and coworkers reported that the reaction of 3-thiapentane-1,5-dithiol with 1,2-dichloroethane in the presence of benzyltrimethylammonium methoxide gave the 2+2 addition product, 18S6 with 32% yield [63], as shown in scheme 1-11.

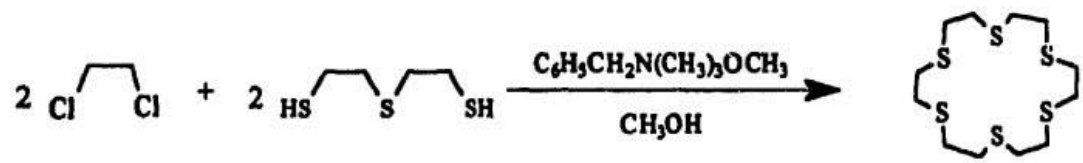

Scheme 1-11

If one of the reactants is a rigid molecule, the

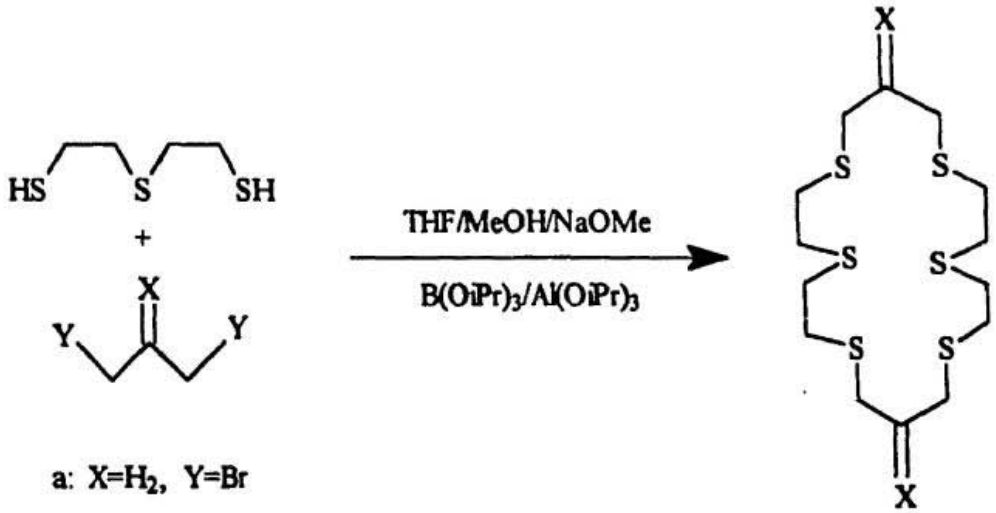

a: $X=H_2$, Y=Br

b: X=O, Y=Cl

c: $X=H_2$, Y=Cl

Scheme 1-12

possibility of 2+2 cyclization is increased [63]. A recent example is the synthesis of crown thioethers in THF/alcohol mixture in the presence of B/Al-alkoxides (Scheme 1-12). This method which requirés rigid functional groups such as ketones and alkenes was discovered by Edema and coworkers [64] and gave high yields (52%) of 2+2 cyclization product.

1.2.2.3. Reactions of Three or More Substrates with Three or More Substrates (3+3,4+4,etc)

The 3+3, 4+4, 5+5, etc. cyclization products are generally by-products either from the high-dilution 1+1 or 2+2

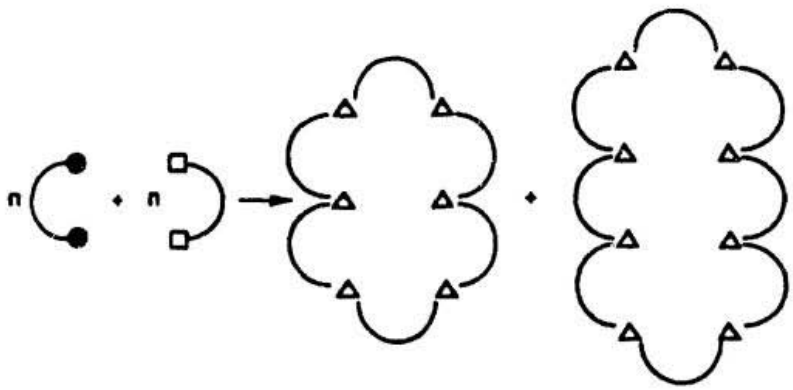

Scheme 1-13

cyclization reactions (Scheme 1-13). These products are isolated by careful chromatography and their yields decrease as the size of ring increases. An example of a 3+3 cyclization reaction is shown by the preparation of 1,4,8,11,15,18-hexathiacycloheneicosane [65] (Scheme 1-14).

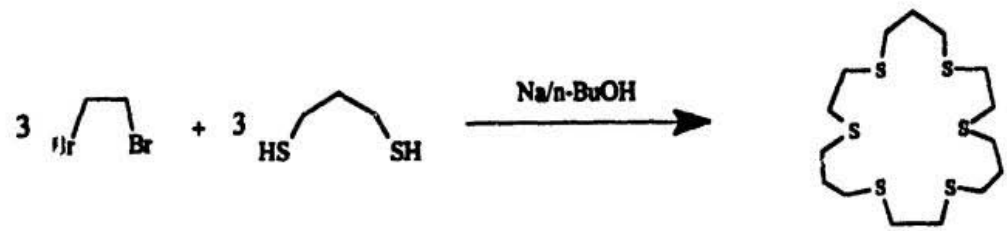

Scheme 1-14

1.2.2.3. Specific Conditions for Ring Closure

One fundamental problem with the preparation of macrocyclic ligands concerns the orientation of reactive sites so that they give macrocyclic products rather than linear polymers. In general, the process of macrocycle formation is preferred by (1) the presence of a metal "template" ion or (2) high dilution conditions.

1.2.2.3.1. Template-Mediated Cyclization Reactions

Sellmmann and Zapf [66,67] discovered the synthesis method involving use of the $Mo(CO)_3$ moiety as a template which affords 9S3 in 60% yield, as shown in Scheme 1-15. Since the starting complex can be regenerated in the reaction cycle, the synthesis is, in principle, performed catalytically.

Sellmmann and coworkers have extended their work on template-mediated synthesis of macrocyclic thioethers [68-70] and have used an $[Fe^{II}(CO)]$ fragment for the synthesis of dibenzo-18S6 and a $[Ru^{II}(CO)]$ for benzo-9S3 respectively (Scheme 1-16).

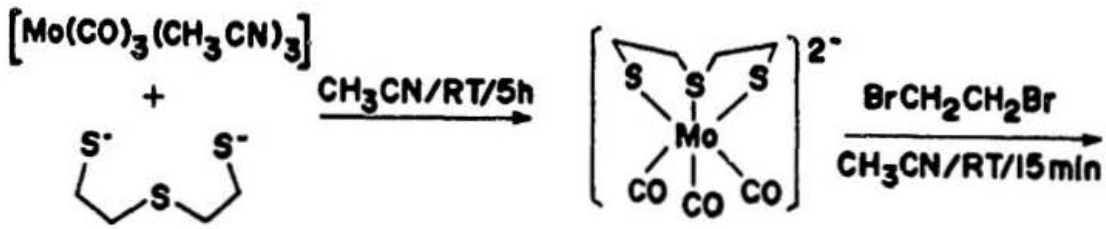

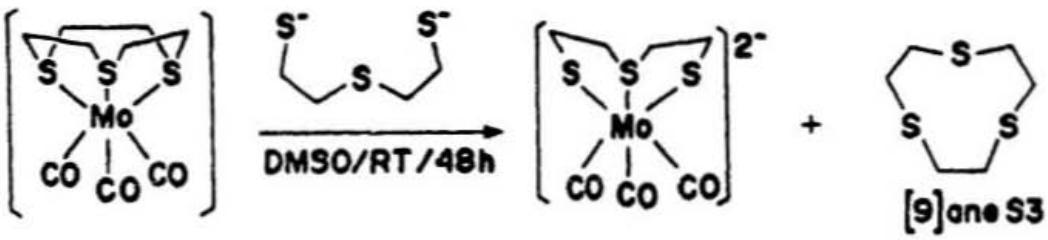

Scheme 1-15

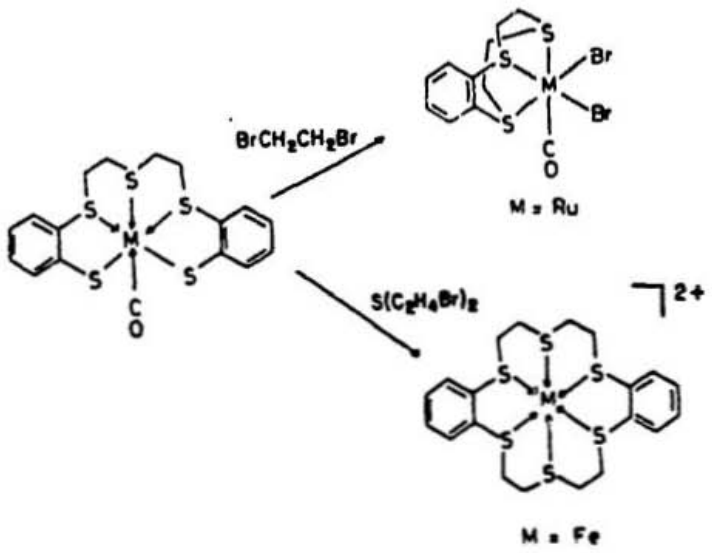

Scheme 1-16

1.2.2.3.2. Use of Cesium Carbonate and High Dilution Conditions

Buter and Kellogg first introduced the use of cesium carbonate to mediate the formation of macrocyclic rings in

1980 [28,29]. Application of this procedure to macrocyclic thioether synthesis greatly diminishes the possibility of polymer formation, with concomitant increase in the yield of the desired macrocyclic products. Use of Cs_2CO_3 coupled with high dilution gives cyclization of α,ω-dithiols and α,ω-dihalides in high yields (typically >75%). The effect of cesium carbonate fostering formation of macrocyclic rings is called the "cesium effect" [71,72].

The smooth cyclization by the Cs_2CO_3/DMF route naturally focusses interest on the critical role of cesium carbonate which clearly surpasses that of other group IA carbonates [29]. A template effect seems to be excluded, because even reactants that lack potential donor groups with affinity for Cs^+ readily yield macrocyclic products. For example, reaction of 1,10-dimercaptodecane with 1,5-dibromopentane gives 1,7-dithiacycloheptadecane in 90% yield [29]. Recently ^{133}Cs NMR studies have indicated that cesium carbonate is nearly or completely dissociated into free ions in dipolar aprotic solvents. Solvents like DMF solvate cations more effectively than anions and as a result, exceptionally nucleophilic thiolate anions are produced. The term "naked anion" has been used to describe these species [72]. High reactivity ensures low concentrations of unreacted starting materials, and fosters high dilution conditions which in turn favours the desired cyclization products.

1.3. Coordination Chemistry of Crown Thioethers

1.3.1. π-Accepting Abilities of crown Thioethers

Thioether ligands, in general, are regarded as σ-donors to metal ion centres [12]. However, a wide range of stable transition metal complexes of crown thioethers has now been reported and this has led to much discussion of the π-acceptor ability of these ligands [11-14].

Several lines of evidence impute appreciable π-accepting abilities to thioethers. Coordination by thioethers typically stabilizes low oxidation states of metal ions, and the lower spin state as well. These phenomena derive largely from the π-acidity of thioethers. This effect clearly appears in electrochemical behaviour. For example, in $[Co(18S6)]^{2+}$ and $[Co(9S3)_2]^{2+}$ complexes, the Co(III/II) couple not only approaches electrochemical reversibility, itself a rarity in cobalt chemistry, but appears at high oxidizing potentials. Comparison with amine complexes is illuminating, in view of the similar ligand field strengths of the two types of ligands. For example, $[Co(9S3)_2]^{2+}$ undergoes oxidation at +680 mV vs NHE [83], whereas $[Co(9N3)_2]^{2+}$ (9N3 is the amine analogue of 9S3) does so at -410 mV vs NHE (in water) [118]. Even allowing for the difference in solvent, these two couples differ by over 1000 mV, which indicates great ability of thioethers to stabilize low oxidation states of metal ions.

Magnetic properties further support π-acidity. Quantitatively, g values reflect π-effects because deviations from g_e (the free electron value) arise from unquenched orbital angular momentum (from circulation of the t_{2g} electrons) [118]. Delocalization of d electrons into an empty orbital of thioethers diminishes the unquenched orbital angular momentum, as measured by the orbital reduction factor k, and thereby the Δg value. For example, in Cu(II) complexes of thioethers the g_{av} values deviate from g_e by less than those from complexes of Cu(II) with harder donor ligands such as H_2O. For $[Cu(18S6)]^{2+}$ and $[Cu(H_2O)_6]^{2+}$, g_{av} is 2.07 and 2.22 respectively [112,119].

Stabilization of the low-spin state also indicates π-interaction in a more dramatic fashion. Delocalization of t_{2g} electron density into empty orbitals of thioethers diminishes electron-electron repulsion and thereby reduces the spin pairing energy. As a consequence, complexes of thioethers, such as $[Co(18S6)]^{2+}$, $[Co(9S3)_2]^{2+}$ and $[Fe(9S3)_2]^{2+}$, typically assume the low-spin state [83,111], like those of phosphines.

Electronic spectral data provide further evidence for π-acidity of thioether ligands. Like the g value, the nephelauxetic ratio β ($\beta = B_{complex}/B_{free\ ion}$, B is the Racah parameter) also measures the delocalizing effect of the ligand [109]. Thioethers allow delocalization of the t_{2g} electron density into their empty orbitals and thereby exhibit a

greater nephelauxetic effect compared to aza donor atoms. This is manifested in a smaller β value in the thioether complexes. For example, β values for $[Ni(9S3)_2]^{2+}$ and $[Ni(10S3)_2]^{2+}$ are 0.66 and 0.69 respectively, while in the corresponding amine complexes $[Ni(9N3)_2]^{2+}$ and $[Ni(10N3)_2]^{2+}$ they are 0.82 and 0.90 respectively [120,121]. The differences in β values reflect greater π-accepting ability of thioethers.

Finally, X-ray structural studies provide direct evidences for π-acidity of thioethers. The single crystal X-ray structure of $[Fe(9S3)_2]^{3+}$ shows a centrosymmetric cation with a mean Fe-S bonding distance equal to 2.280(3) Å [82]. This Fe-S bond length is longer than that obtained from $[Fe(9S3)_2]^{2+}$ which shows a mean Fe-S bonding distance of 2.250(1) Å [81]. The elongation in Fe-S bonds on going from Fe^{2+} to Fe^{3+} gives direct structural evidence for the π-accepting properties of crown thioethers. Thus, loss of an electron from a formally bonding t_{2g} orbital leads to a decrease in π-back-bonding from Fe→S and to a lengthening of Fe-S bond length. In contrast, in the absence of π-acidity, increasing the cation charge (from 2+ to 3+) and decreasing the ionic radius of the metal centre (from 0.61 Å for Fe^{2+} to 0.55 Å for Fe^{3+} [122]) would be expected to decrease the Fe-S bond lengths on oxidation of $[Fe(9S3)]^{2+}$ to $[Fe(9S3)]^{3+}$. A similar observation has been obtained for the trans-

$[MoBr_2(Me_8[16]aneS_4)]^{+1/0}$ couple ($Me_8[16]aneS_4$=3,3,7,7,11,11,15,15-octamethyl-1,5,9,13-tetrathiacyclohexadecane) [123]. The Mo-S bond lengths for trans-$[MoBr_2(Me_8[16]aneS_4)]^+$ (mean Mo-S 2.502(5) Å) are significantly longer than those in trans-$[MoBr_2(Me_8[16]aneS_4)]$ (mean Mo-S 2.436(2) Å). These structural results lend strong support to the π-accepting ability of thioethers.

The conventional explanation of π-back-bonding for the third row elements makes use of the fact that they possess empty 3d orbitals, which might have the right symmetry and energy to undergo additional bonding interaction [124,125]. Though this is a fruitful concept, recent theoretical studies cast doubt on it as the sole explanation.

For example, tertiary phosphines, PR_3, have traditionally been regarded as good π-acceptor ligands due to the empty 3d orbitals on the P atom [126]. Theoretical studies by Trogler [127] and by Marynick [128], however, showed that these orbitals are too high in energy to reasonably interact with a metal centre. It is suggested that P-R σ* orbitals function as the acceptor orbitals instead, and this was supported by Orpen and Connelly with structural evidence [129]. Prompted by these calculations, Ziegler and coworkers studied thioethers SR_2, and obtained the similar results. Their calculations suggest it is a low-lying S-R σ* orbital of the thioether that accepts electron density from the metal centre

[130]. These hypotheses remain to be verified experimentally.

In summary, during coordination to metal ions thioethers can act as both σ-donors and π-acceptors. Though they are relatively weak ligands compared to phosphines, both experimental evidence and molecular orbital calculations support the ability of thioethers to serve as π-acceptors.

1.3.2. Ligand Conformation

Structural work on macrocyclic thioethers reveals an interesting property. The crown thioethers generally adopt "exodentate" conformations with their S-donors pointing out of their macrocyclic cavities [73,74]. In contrast, the endodentate orientation is commonly found in oxa and aza macrocycles [75]. This difference in ring conformation originates in the conformational preference of the constituent bonds, and it has an important effect on the coordination chemistry of crown thioethers. Exodentate S atoms necessitate rearrangement from exo to endo conformation before chelation can occur. This change is accompanied by a corresponding enthalpic cost. As a consequence, some crown thioethers tend to bridge metal ions rather than chelate to just one [76]. Not all crown thioethers, however, adopt exodentate conformations. For example, 9S3 has endodentate orientation of all three S atoms [77].

Crown thioethers commonly manifest these exodentate conformations because C-S-C-C units slightly prefer gauche placement, whereas S-C-C-S fragments strongly prefer the anti conformation [78]. These preferences originate at least in part from the difference in 1,4-interactions at C-S and C-C bonds. As a result, S-C-C-S systems disfavour gauche placement relative to O-C-C-O species. In ethylene-linked crown thioethers, $(SCH_2CH_2)_n$, (n>3), the conformational preferences of both C-S and C-C bonds act in concert to generate "bracket" S-C-C-S-C-C-S units, in which the central S atom marks a corner, as shown in Scheme 1-17. Such bracket units form the fundamental building block of crown thioethers. For example, 12S4 results from fusion of two such units and has four corner S atoms [78].

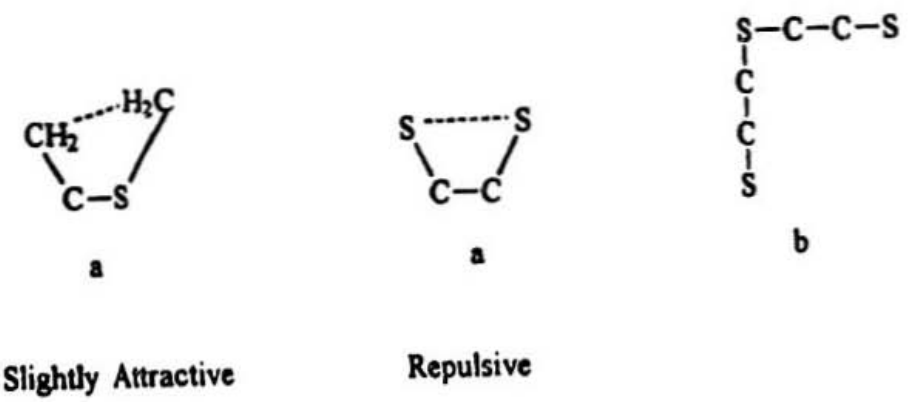

Scheme 1-17. (a) 1,4-interactions in gauche placements
(b) a S-C-C-S-C-C-S bracket unit

1.3.3. Coordination Chemistry of 9S3

Among the crown thioethers, 1,4,7-trithiacyclononane [9]aneS$_3$ (9S3) **1** , in particular, usually binds facially to metal ions and therefore parallels the coordination of cyclopentadienyl, aryl, and tripyrazolylborate. X-ray structure studies reveal that 9S3 retains its conformation on binding to a metal centre [15,77]. In fact, the enthalpic price for arranging the donor atoms for coordination is paid in the synthesis of the ligand. This retention of conformation confers unique stability on chelating 9S3 complexes. Owing to its powerful chelating ability 9S3 forms a great variety of transition metal complexes, and is now the most extensively studied of crown thioethers. These works have been reviewed by Cooper and Schröder [14,15].

Classified by Periodic Row, the complexes of 9S3 are summarized in Tables 1-1 to 1-3.

1.3.4. Coordination Chemistry of 18S6

A hexadentate ligand can yield either of two isomeric octahedral complexes of meso or racemic stereochemistry (Fig. 1-1) [9,10]. In all encapsulated complexes reported to date, 1,4,7,10,13,16-hexathiacyclooctadecane [18]aneS$_6$ (18S6) **2**

Table 1-1. [9]aneS$_3$ (9S3) Complexes of First-row Metals

Metal Cation	Other Ligands	Complex	Coordination Geometry	Remarks	Refs.
Cr^{3+}		$[Cr(9S3)_2]^{3+}$	octahedral	elemental analysis and electronic spectra	[79]
Cr^{3+}	Cl	$[CrCl_3(9S3)]^{3+}$			[79]
Mn	CO	$[Mn(CO)_3(9S3)]$	octahedral	X-ray structure data	[80]
Fe^{2+}		$[Fe(9S3)_2]^{2+}$	octahedral	X-ray structure data; low spin	[81]
Fe^{3+}		$[Fe(9S3)^2]^{3+}$	octahedral	Fe-S bond lengths shorter than those in $[Fe(9S3)_2]^{2+}$; low spin	[82]
Co^{2+}		$[Co(9S3)_2]^{2+}$	octahedral	low spin; X-ray structure data	[83]
Co^{3+}		$[Co(9S3)_2]^{3+}$	octahedral	X-ray structure data	[84]
Ni^{2+}		$[Ni(9S3)_2]^{2+}$	octahedral	X-ray structure data	[85]
Ni^{3+}		$[Ni(9S3)_2]^{3+}$	octahedral	X-ray structure data	[86]

Table 1-1. (continued)

Metal Cation	Other Ligands	Complex	Coordination Geometry	Remarks	Refs.
Cu^{+}	I	$[CuI(9S3)]$	tetrahedral	X-ray structure data	[85]
Cu^{+}	PPh_3	$[Cu(PPh_3)(9S3)]^{+}$	tetrahedral	X-ray structure data	[86]
Cu^{+}	$AsPh_3$	$[Cu(AsPh_3)(9S3)]^{+}$	tetrahedral	X-ray structure data	[86]
Cu^{+}		$[Cu(9S3)_2]^{+}$	tetrahedral	[3+1] coordination	[87]
Cu^{+}		$[Cu_2(9S3)_3]^{2+}$	tetrahedral	one 9S3 molecule bridging two [Cu(9S3)] moieties	[90]
Cu^{2+}		$[Cu(9S3)_2]^{2+}$	octahedral	X-ray structure data	[83,88]
Cu^{2+}	Cl	$[CuCl_2(9S3)]$	square pyramid	X-ray structure data	[89]

Table 1-2. [9]aneS$_3$ (9S3) Complexes of Second-row Metals

Metal Cation	Other Ligands	Complex	Coordination Geometry	Remarks	Refs.
Mo	CO	[Mo(CO)(9S3)]	octahedral	X-ray structure data	[91]
Ru^{2+}		$[Ru(9S3)]^{2+}$	octahedral	very stable; X-ray structure data	[92-94]
Ru^{2+}	Cl; PPh_3	$[RuCl_2(PPh_3)(9S3)]$	octahedral	X-ray structure data	[95]
Rh^{2+}		$[Rh(9S3)_2]^{2+}$	octahedral	EPR; CV	[96,97]
Rh^{3+}		$[Rh(9S3)_2]^{3+}$	octahedral	X-ray structure data	[96-97]
Rh^{2+}	C_5Me_5	$[Rh(C_5Me_5)(9S3)]^+$		mixed-sandwich structure	[13]
Pd^{2+}	Br	$[PdBr_2(9S3)]$	square pyramidal	X-ray structure data	[98]
Pd^{2+}		$[Pd(9S3)_2]^{2+}$	square plane	X-ray structure data	[98,99]
Pd^{3+}		$[Pd(9S3)_2]^{3+}$	octahedral	Pd-S_{axial} much longer than Pd-S_{equ} (by 0.64 Å)	[99]
Ag^+		$[Ag(9S3)_2]^+$	octahedral	X-ray structure data	[100]
Ag^{2+}		$[Ag(9S3)_2]^{2+}$	octahedral	EPR; electronic spectroscopy	[81]
Ag^+		$[Ag_3(9S3)_3]^{3+}$	tetrahedral	trimer; Ag(I) bridged by 9S3	[85]
Cd^{2+}	I	$[CdI_2(9S3)]_2$	octahedral	dimer; two I bridging two [CdI(9S3)]moities	[101]

Table 1-3. [9]aneS (9S3) Complexes of Third-row Metals

Metal Cation	Other Ligands	Complex	Coordination Geometry	Remarks	Refs.
Tc^{2+}		$[Tc(9S3)_2]^{2+}$	octahedral	X-ray structure data	[38]
Re^{+}	CO	$[Re(CO)_3(9S3)]^{+}$	octahedral	X-ray structure data	[102]
Pt^{2+}		$[Pt(9S3)_2]^{2+}$	square pyramidal	X-ray stucture data	[103]
Pt^{+}	Me	$[Pt(Me_3)(9S3)]^{+}$	octahedral	X-ray structure data	[104]
Au^{+}		$[Au(9S3)_2]^{+}$	Tetrahedral	[3+1] coordination	[105]
Au^{2+}		$[Au(9S3)_2]^{2+}$	octahedral	X-ray structure data	[106]
Hg^{2+}		$[Hg(9S3)_2]^{2+}$	octahedral	X-ray structure data	[107]

Table 1-4. [18]aneS$_6$ (18S6) Complexes

Metal Cation	Other Ligands	Complex	Coordination Geometry	Remarks	Refs.
Fe^{2+}		$[Fe(18S6)]^{2+}$	octahedral	X-ray structure data	[108]
Ni^{2+}		$[Ni(18S6)]^{2+}$	octahedral	X-ray structure data	[109,110]
Co^{2+}		$[Co(18S6)]^{2+}$	octahedral	X-ray structure data	[111]
Cu^{+}		$[Cu(18S6)]^{+}$	tetrahedral	X-ray structure data	[112]
Cu^{+}	MeCN	$[(CuMeCN)_2(18S6)]^{2+}$	tetrahedral	two $[Cu(MeCN)S_3]$ units	[113]
Cu^{2+}		$[Cu(18S6)]^{2+}$	octahedral	X-ray structure data	[112]
Rh^{2+}	C_5Me_5	$[(Rh(C_5Me_5)Cl)_2(18S6)]$		two $[Rh(C_5Me_5)ClS]$ units	[114]
Pt^{2+}		$[Pt(18S6)]^{2+}$	square plane	X-ray structure data	[115]
Pd^{2+}		$[pd(18S6)]^{2+}$	square plane	X-ray structure data	[115]
Au^{+}		$[Au(18S6)]^{+}$	octahedral	X-ray structure data	[116]
Ag^{+}		$[Ag(18S6)]^{+}$	octahedral	X-ray structure data	[117]

coordinates in the centrosymmetric meso form. This arises from the conformational propensity of C-S-C-C linkages to adopt gauche placement. In the meso isomer all 12 C-E-C-C groups assume gauche placement, whereas in an isomeric racemic structure, only 8 of the 12 do so.

Fig. 1-1

The complexes of 18S6 are summarized in Table 1-4.

1.4. Reference

1. Mansfeld, W, Ber. *19*, 696 (1886).
2. Ray, P.C., J. Am. Chem. Soc., *11*, 1090 (1920).
3. Ray, P.C., J. Chem. Soc.,*121*, 1279 (1922).
4. Ray, P.C., J. Chem. Soc.,*123*, 2174 (1923).
5. Bennett, G.M., J. Chem. Soc., *121*, 2139 (1922).
6. Bennett, G.M.; Berry, W.A., J. Chem. Soc., *127*, 910 (1925).

7. Mendow, J.R.; Reid, E.E., J. Am. Chem. Soc., *56*, 2177 (1934).

8. Pederson, C.J., J. Am. Chem. Soc., *89*. 7017 (1967).

9. Black, D.S.C.; McLean, I.A., Tetrahedron Lett., 3961 (1969).

10. Black, D.S.C.; McLean, I.A., Aust. J. Chem., *24*, 1401 (1971).

11. Cooper, S.R., Acc. Chem. Rev., *21*, 141 (1988).

12. Murray, S.G.; Hartley, F.R., Chem. Rev., *81*, 365 (1981).

13. Schröder, M., Pure Appl. Chem., *60*, 517 (1988).

14. Blake, A.J.; Schröder, M., Adv. Inorg. Chem, *35*, 1 (1990).

15. Cooper, S.R.; Rawle, S.C., Struct. and Bonding, *72*, 1 (1990).

16. Margerum, D.W.; Smith, G.F., J. Chem. Soc., Chem. Commun., 807 (1975).

17. Cabbiness, D.K.; Margerum, D.W., J. Am. Chem. Soc., *91*, 6540 (1969).

18. McCormick, D.B.; Griesser, R. and Sigel, H., Met. Ions Biol. Syst., *1*, 213 (1973).

19. Solomon, E.I.; Penfield, K.W.; Wilcox, D.E., Struct. and Bonding, *53*, 1 (1983).

20. Collman, P.M.; Freeman, H.C.; Guss, J.M.; Murata, V.A.; Norris, V.A.; Ramshaw, J.A.M.; Venkatappa, M.P., Nature (London), *272*, 319 (1978).

21. Guss, J.M.; Freeman, H.C., J. Mol. Biol, *169*, 521 (1978).

22. Beinert, H., Coord. Chem. Rev., *33*, 55 (1980).

23. Vallee, B.L.; Williams, R.J.P., Biochemistry, 59, 498 (1986).

24. Williams, R.J.P., J. Mol. Cat., 1 (1986).

25. Chatt, J.; Leigh, G.J.; Storace, A.P., J. Chem. Soc., A, 1380 (1971).

26. Lemke, W.; Travis, K.; Takvoryan, N.; Bush, D.H., Adv. Chem. Ser., *150*, 358 (1976).

27. Ochrymowycz, L.A.; Gerber, D.; Chong, S.R.; Leung, A.K., J. Org. Chem., *42*, 2644 (1977).

28. Buter, J., Kellogg, R.M., J. Chem. Soc., Chem. Commun., 466 (1980).

29. Buter, J.; Kellogg, R.M., J. Org. Chem., *46*, 4481 (1981).

30. Livingstone, S.E., Quart. Rev., Chem. Soc., *19*, 386 (1965).

31. Hung, Y.; Martin, L.Y.; Jackels, S.C.; Tait, A.M.; Busch, D.H., J. Am. Chem. Soc., *99*, 4029 (1977).

32. Martin, L.Y.; Sperati, C.R.; Bush, D.H., J. Am. Chem. Soc., *99*, 2967 (1977).

33. Martin, L.Y.; Dehayes, L.J.; Zompa, L.J.; Bush, D.H., J. Am. Chem. Soc., *96*, 4046 (1974).

34. Martell, A.E., Inorganic Chemistry in Biology and

Medicine, Vol. 140, ACS Symposium Series, American Chemical Society, Wahington, DC, P91-119 (1980).

35. Charke, M.J.; Podbielski, L., Coord. Chem. Rev., *75*, 253 (1987).
36. Pinkerton, T.C.; Desilets, C.P.; Hoch, D.J.; Mikelsons, M.V.; Wilson, G.M.J., J. Chem. Educ., *62*, 965 (1985).
37. Dentsch, E.; Bushong, W.; Glavan, K.A.; Elder, R.C.; Sodd, V.J.; Scholz, K.L.; Fortman, D.L.; Lakes, S.J., Science, *214*, 85 (1981).
38. White, D.J.; Küppers, H.J.; Edwards, A.J.; Walkin, D.J.; Cooper, S.R., Inorg. Chem., *31*, 5351 (1992).
39. Moyer, B.A.; Westerfield, C.L.; McDowell, W.J.; Case, G.N., Sep. Sci. Technol., *23*, 100 (1988).
40. Sekido, E.; Kawahara, H.; Tsuji, k., Bull. Chem. Soc. Jap., *61*, 1587 (1988).
41. Oue, M.; Kimura, K.; Shono, T., Anal. Chim. Acta, *194*, 293 (1987).
42. Buter, J.; Kellogg, R.M., and van Bolhuist, F., J. Chem. Soc., Chem. Commun., 282 (1990).
43. Kellogg, R.M.; Kapteina, B. and Buter, J., Bull. Soc. Chim. Belg., *99*, 703 (1990).
44. Vriesema, B.K.; Lemaire, M.; Buter, J.; Kellogg, R.M., J. Org. Chem., *51*, 5169 (1986).
45. Kellogg, R.M., Angew. Chem, Int. Ed. Engl., *23*, 782 (1984).

46. Cross, G.; Vriesema, B.K.; Boven, G.; Kellogg, R.M.; van Bolhuis, F., J. Organomet. Chem., *370*, 357 (1989).

47. Jorgensen, T.; Hansen, T.K. and Becher, J., Chem. Rev., 41 (1994).

48. Ferraris, J.P.; Cowan, D.O.; Walatka, V. and Perlstein, J.H., J. Am. Chem. Soc., *95*, 948 (1973).

49. Newkome, G.R.; Moorefield, C.N.; Baker, G.R., Behera, R.K.; Escamilia, G.H.; Saunders, M.T., Angew. Chem. Int. Ed. Engl., *31*, 917 (1992).

50. Gasiorowski, R.; Jorgensen, T.; Moller, J.; Hansen, T.K.; Pietraszkiewicz, M.; Becher, J., Adv. Mat., *4*, 568 (1992).

51. Jorgensen, T.; Girmay, B.; Hamsen, T.K.; Becher, J.; Underhill, A.E.; Hursthouse, M.B.; Harman, M.E.; Kilburn, J.D., J. Chem. Soc. Perkin Trans., 1, 2907 (1992).

52. Tachikawa, T.; Iznoka, A. and Sngawara, T., J. Chem. Soc., Chem. Commun., 1227 (1993).

53. Cossar, B.C, Fournier, J.O.; Field, D.L.; Reynolds, D.D., J. Org. Chem., *27*, 93 (1962).

54. Speziale, A.J., Org. Syn. Coll., IV, 401 (1963).

55. Martin, D.J.; Greco, C.C., J. Org. Chem., *33*, 1275 (1968).

56. Partyka, R.A.; U.S. Patent, 3,290,319 (1966); Chem. Abstr., *66*, 115609k (1967).

57. Buter, J. and Kellogg, R.M., Org. Synth., *65*, 150 (1987).

58. Ziegler, K.; Eberle, H and Ohlinger, H., Liebigs Ann. Chem., *504*, 95 (1933).

59. Blower, P.J.; Cooper, S.R., Inorg. Chem., *26*, 2009 (1987).

60. Wolf, R.E.; Hartman, J.R.; Ochrymowycz, L.A.; Cooper, S.R., Inorg. Synth., *25*, 123 (1989).

61. McAuley, A.; Subramanian, S., Inorg. Chem., *29*, 2830 (1990).

62. Rossa, L. and Vögtle, F., Synthesis of Medio and Macrocyclic Compounds by High Dilution Priciple Techniques, Boschlee, F.L. Ed., Springer-Verlag, Berlin (Transl. of Topic Curr. Chem., 113), 1983.

63. Blake, A.J.; Greig, J.A. and Schroder, M., Angew. Chem. Int. Ed. Engl., *25*, 274 (1986).

64. Edema, J.J.H.; Stock, H.T.; Buter, J.; Kellogg,R.M.; Smeets, W.J.J.; Spek, A.L.; Bolhuis, F.V., Angew. Chem. Int. Ed. Engl., *32*, 436 (1993).

65. Ochrymowycz, L.A.; Mak, C.P.; Michna, J.D., J. Org. Chem., 2079 (1974).

66. Sellman, D.; Zaph, L., Angew. Chem. Int. Ed. Engl., *23*, 808 (1984).

67. Sellman, D.; Zaph, L., J. Organomet. Chem., *289*, 57 (1986).

68. Sellman, D.; Frank, P., Angew. Chem. Int. Ed. Engl., *25*, 1107 (1986).

69. Sellman, D.; Frank, P.; Knoch, F.J., J. Organomet. Chem., *339*, 345 (1988).

70. Sellman, D.; Knoch, F.J.; Wronna, C., Angew. Chem. Int. Ed. Engl., *27*, 691 (1988).

71. Bradshaw, J.S.; Krakowiak, K.E; Izatt, R.M., Aza-crown Macrocycles, The Chemisty of Heterocyclic Compounds, Vol. 51, John Wiley & Sons, Inc., New York, P101 (1993).

72. Dijkstra, G.; Kruizinga, W.H.; Kellogg, R.M., J. Org. Chem., *52*, 4230 (1987).

73. Desimone, R.E.; Glick, M.D., J. Am. Chem. Soc., 98, 762 (1976).

74. Dalley, N.K.; Larson, S.B.; Smith, J.S.; Matheson, K.L.; Izatt, R.M.; Christensen, J.J., J. Heterocycl. Chem., *18*, 463 (1981).

75. Dalley, N.K., Synthetic Multidentate Macrocyclic Compounds, Izatt, R.M.; Christensen, J.J., Eds., Academic Press, New York, P207 (1978).

76. Blake, A.J.; Taylor, A.; Schröder, M., J. Chem. Soc., Chem. Commun., 1097 (1993).

77. Glass, R.S.; Wilson, G.S.; Setzer, W.N., J. Am. Chem. Soc., *102*, 5068 (1980).

78. Wolf, R.E.; Hartman, J.R.; Storey, J.M.E.; Foxman, B.M., Cooper, S.R., J. Am. Chem. Soc., *109*, 4328 (1987).

79. Küppers, H.J.; Wieghardt, K., Polyhedron, *8*, 1770 (1989).

80. Elias, H.; Schmidt, G.; Küppers, H.J.; Saher, M.; Wieghardt, K.; Nüber, B.; Weiss, J., Inorg. Chem., *28*, 3021 (1989).

81. Küppers, H.J.; Wieghardt, K.; Nüber, B.; Weiss, J.; Bill, E.; Trautwein, A.X., Inorg. Chem., *26*, 3762 (1987).

82. Blake, A.J.; Holder, A.J.; Hyde, T.I.; Schröder, M., J. Chem. Soc., Chem. Commun., 987 (1989).

83. Setzer, W. N.; Ogle, C.A.; Wilson, G.S.; Glass, R.S., Inorg. Chem., *22*, 266 (1983).

84. Küppers, H.J.; Neves, A.; Pomp, C.; Ventur, D.; Wieghardt, K.; Nuber, B.; Weiss, J., Inorg. Chem., *25*, 2400 (1986).

85. Küppers, H.J.; Wieghardt, K.; Tsay, Y.H.; Krüger, C.; Nüber, B.; Weiss, J., Angew. Chem. Int. Ed. Engl., *26*, 575 (1987).

86. Blake, A.J.; Gould, R. O.; Halcrow, M.A.; Holder, A.J.; Hyde, T.Z.; Schröder, M., J. Chem. Soc., Dalton Trans., *24*, 3427 (1992).

87. Kano, S.K.; Glass, R.S.; Wilson, G.S., J. Am. Chem. Soc., 115, 592 (1993).

88. Glass, R.S.; Steffen, L.K.; Swanson, D.D.; Wilson, G.S.; Gelder, R.; Graaff, R.A.G.; Reedijk, J.; Inorg. Chim.

89. Shen, J.; Pichardt, J., Z. Naturforsch, *47B*, 1736 (1992).

90. Clarkson, J.A.; Yagbasan, R.; Blower, P.J.; Cooper, S.R., J. Chem. Soc., Chem. Commun., 1244 (1989).

91. Ashby, M.T.; Lichtenberger, D.L., Inorg. Chem., *24*, 636 (1985).

92. Rawle, S.C.; Cooper, S.R., J. Chem. Soc., Chem. Commun. 308 (1987).

93. Rawle, S.C.; Sewell, T.J.; Cooper, S.R., Inorg. Chem., *26*, 3769 (1987).

94. Bell, M.N.; Blake, A.J., Schröder, M.; Küppers, H.J.; Wieghardt, K., Angew. Chem. Int. Ed. Engl., *26*, 250 (1987).

95. Alcock, N.W.; Cannadine, J.C.; Clark, G.R.; Hill, A.F., J. Chem. Soc., Dalton Trans., 1131 (1993).

96. Blake, A.J.; Gould, R.O.; Holder, A.J.; Hyde, T.I., Schröder, M.,J. Chem. Soc., Dalton Trans., 1861 (1988).

97. Rawle, S.C.; Yagbasan,R.; Prout, K.; Cooper. S.R., J. Am. Chem. Soc., *109*, 6181 (1987).

98. Wieghardt, K.; Küppers, H.J.; Raabe, E.; Kruger, C., Angew. Chem. Int. Ed. Engl., *25*, 1101 (1986).

99. Blake, A.J.; Holder, A.J.; Hyde, T.I.; Roberts, Y.V.; Lavery, A.J.; Schröder, M., J. Organomet. Chem., *323*, 261 (1987).

100. Blower, P.J.; Clarkson, J., Rawle, S.C.; Hartman, J.R.;

100. Blower, P.J.; Clarkson, J., Rawle, S.C.; Hartman, J.R.; Wolf, R.E. Jr; Yagbasan, R.; Bott, S.G.; Cooper, S.R., Inorg. Chem., *28*, 4040 (1989).

101. Pickart, J.; Shen, J., Z. Naturforsch., *B48*, 969 (1993).

102. Pomp, C.; Drueke, S.; Küppers, H.J.; Wieghardt, K.; Kruger, C.; Nüber, B.; Weiss, J., Z. Naturforsch., *B43*, 299 (1988).

103. Blake, A.J.; Geig, J.A.; Holder, A.J.; Hyde, T.I.; Taylor, A.; Schröder, M., Angew. Chem. Int. Ed. Engl., *29*, 197 (1990).

104. Abel, E.W.; Beer, P.D.; Moss, I.; Orrell, K.G.; Sik, V.; Bates, P.A.; Hursthouse, M.B., J. Chem. Soc, Chem. Commun., 978 (1987).

105. Blake, A.J.; Gould, R.O.; Holder, A.J.; Hyde, T.I.; Taylor, A.; Schröder, M., J. Chem. Soc, Chem. Commun., 876 (1989).

106. Blake, A.J.; Greig, J.A.; Holder, A.J.; Hyde, T.I.; Taylor, A.; Schröder, M., Angew. Chem. Int. Ed. Engl., *29*, 197 (1990).

107. Parker, D.; Roy, P.S.; Ferguson, G.; Hunt, M.M., XXVI International Conference on Coordination Chemistry, Porto, Portugal, August 1988, abstract B4.

108. Grant, G.J.; Isaac, S.M.; Setzer, W.N.; Vanderveer, D.G., Inorg. Chem., *32*, 4284 (1993).

Admans, G.A., Inorg. Chem., *27*, 1209 (1988).

110. Hintsa, E.J.; Hartman, J.R.; Cooper, S.R., J. Am. Chem. Soc., *105*, 3738 (1983).

111. Shannon, R.D., Acta Crystallogr., *A32*, 751 (1976).

112. Hartman, J.R.; Cooper, S.R., J. Am. Chem. Soc., *108*, 1202 (1986).

113. Gould, R.O.; Lavery, A.J.; Schröder, M., J. Chem. Soc., Chem. Commun., 1492 (1985).

114. Bell, M.N.; Blake, A.J.; Schröder, M., J. Chem. Soc., Chem. Commun., 471 (1986).

115. Blake, A.J.; Gould, R.O.; Lavery, A.J.; Schröder, M., Angew. Chem. Int. Ed. Engl., *25*, 274 (1986).

116. Blake, A.J.; Gould, R.O.; Holder, A.J.; Hyde, T.I.; Schröder, M., J. Chem. Soc., Chem. Commun., 1097 (1993).

117. Blake, A.J.; Gould, R.O.; Holder, A.J.; Hyde, T.I.; Schröder, M., Polyhedron, *8*, 513 (1989).

118. Wieghardt, K.; Schmidt, W.; Herrmann, W.; Küppers, H.J., Inorg. Chem., 22, 2953 (1983).

119. Bleaney, B.; Bowers, K.D.; Proc. R. Soc. (London), *A228*, P157-166 (1955).

120. Wieghardt, K.; Küppers, H.J. and Weiss, J., Inorg. Chem., *24*, 3067 (1985).

121. Chandrasekhar, S.,; McAuley, A., Inorg. Chem., *31*, 2234 (1992).

122. Shanon, R.D., Acta Crystallogr., A, *32*, 751 (1976).

123. Adachi, T.; Durrant, M.D.; Hughes, D.L.; Pickett, C.J.; Richards, R.L.; Talarmin, J.; Yoshida, T., J. Chem. Soc., Chem. Commun., 1464 (1992).

124. Huheey, J.E., Inorganic Chemistry, 3 Ed., Harper & Row, Cambridge, P824 (1983).

125. Kuehn, C.G.; Isied, S.S., Prog. Inorg. Chem., *27*, 153 (1980).

126. Collman, J.P.; Hegedus, L.S.; Norton, J.R.; Finke, R.G., Principles and Applications of Organotransition Metal Chemistry, University Science Books, Mill Valley, CA, P66 (1987).

127. Xiao, S.X.; Trogler, W.C.; Ellis, D.E.; Berkovich-Yellin, Z., J. Am. Chem. Soc., *105*, 7033 (1983).

128. Marynick, D.S., J. Am. Chem. Soc., *106*, 4064 (1984).

129. Orpen, A.G.; Connelly, N.G., J. Chem. Soc., Chem. Commun., 1310 (1985).

130. Jacobsen, H.; Kraatz, H.Z.; Ziegler, T. and Boorman, P.M., J. Am. Chem. Soc., *114*, 7851 (1992).

II. Syntheses and Characterization of 1-Oxa-4,7-dithiacyclononane ([9]aneOS$_2$) and 1,10-Dioxa-4,7,13,16-tetrathiacyclooctadecane([18]aneO$_2$S$_4$)

2.1. Introduction

Crown thioethers have been extensively used in recent years to study transition metal complexes. Among them [9]aneS$_3$ **1** has attracted special attention [1,2]. [9]aneS$_3$ is unique in retaining its endo-conformation on binding to a trigonal face of a metal. This retention of conformation confers unusual stability on [9]aneS$_3$ complexes of metal ions in uncommon oxidation states, such as, for example, Pd(III), Pt(III), and Ag(II) [3-5].

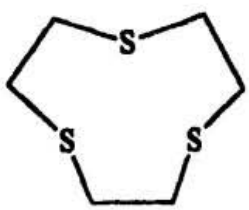

1

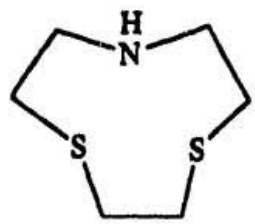

2

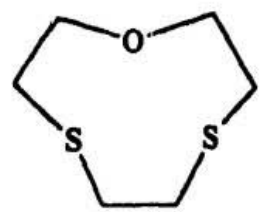

3

The nine-membered tridentate ligand ring 7-aza-1,4-dithiacyclononane([9]aneNS$_2$) **2** and the structures of its nickel and palladium complexes have been reported recently [6,7]. The electronic spectra of its Ni(II) complexes indicate [9]aneS$_3$ exerts a considerably stronger ligand field than does [9]aneNS$_2$. Molecular mechanics calculations have also been carried out for several related nine-membered ring systems [8].

No reports are available on [9]aneOS$_2$ **3**. Interest in this mixed donor ligand stems from the fact that it contains both a hard O-donor and soft S-donors which could give a coordination environment around metal centres similar to that in metalloenzymes such as blue copper-containing oxidases [9]. Therefore, for possible modelling of the active sites of proteins, we have synthesized [9]aneOS$_2$ and investigated its complexing properties, and have compared them with those of other nine-membered ligands, such as **1** and **2**.

2.2. Experimental Section

All commercially available reagents were obtained from the Aldrich Chemical Co. Inc. or from Morton Thiokol Alfa Products Inc. and were used without further purification. Spectroscopic data were obtained by using the following instruments: IR, Mattson Polaris FT; NMR, General Electric 300-NB; mass spectra, V.G. Micromass 7070HS. Analyses were performed by Canadian

Microanalytical Service Ltd.

2.2.1. Preparation of 1-Oxa-4,7-dithiacyclononane([9]aneOS$_2$) and 1,10-Dioxa-4,7,13,16-tetrathiacyclooctadecane([18]aneO$_2$S$_4$)

Cesium carbonate (14.5 g, 45 mmol) was dried in an oven at 80°C for 10 h and finely powdered, and then transferred to a 2L three-necked flask equipped with a mechanical stirrer. N,N-dimethylformamide (DMF) (300 mL, from a freshly opened bottle) was deaerated under suction and then transferred to the 2L reaction flask. The reaction mixture was stirred vigorously to keep the cesium carbonate as a fine suspension. The temperature of the reaction mixture was maintained at 80°C. A solution of 2-mercaptoethyl ether (4.9 g, 36 mmol) and 1,2-dibromoethane(6.7 g, 36 mmol) in the deaerated DMF (300 mL) was added from a dropping funnel at the rate of 6-8 mL/h under a nitrogen atmosphere. After the addition was complete, stirring was continued at 80°C for a further 12 h.

At the end of reaction, DMF was removed by using a rotary evaporator. The yellow residue was suspended in 100 mL of water and extracted with 3x100 mL of dichloromethane. The combined extracts were washed with 1.0 mol L^{-1} aqueous NaOH (100 mL) and then water (2x100 mL), and dried over anhydrous sodium sulfate. After removing the solvent, ethanol (200 ml) was added to the brown viscous mixture and the mixture was filtered.

The filtrate was concentrated to a brown oil by using a rotary evaporator. The product [9]aneOS$_2$ was collected by vacuum distillation, b.p. 85-90°C/0.5mm.; yield 2.3g (39%). IR (cm^{-1}, KBr, Nujol): 2910(s), 2854(s), 1462(m), 1407(s), 1359(m), 1294(s), 1272(s), 1190(m), 1119(vs), 1042(m), 911(m), 838(m), 767(w), 674(w), 459(m); ^{1}H NMR (ppm from TMS internal standard, $CDCl_3$): 3.95(t,9.6Hz,4H),-CH_2O; 3.07(s,br,4H),-SCH_2CH_2S-; 2.80(t,9.6Hz,4H),-CH_2S. ^{13}C NMR ($CDCl_3$): 73.7,-CH_2O; 34.6,SCH_2-; 33.2,$(CH_2S)_2$. High resolution mass spectral data: calcd for $C_6H_{12}OS_2$: m/e 164.0329(M$^+$); found: m/e 164.0330(M$^+$).

The brown solid separated by filtration was dissolved in hot ethanol (400 mL) and decolourized with activated charcoal. The solution was filtered while hot. A white needle-like crystalline solid ([18]aneO$_2$S$_4$) was formed after cooling; yield 0.5g (8.4%). Recrystallization from dichloromethane afforded colourless crystals suitable for X-ray diffraction. Mp: 124-125°C (lit. 125-126°C [10]). IR (cm^{-1}, KBr, Nujol): 2923(vs), 2855(vs), 1460(s), 1377(m), 1298(m), 1230(m), 1115(m), 1045(m), 1004(w), 942(w), 798(w), 722(w), 705(w), 650(vw). ^{1}H NMR ($CDCl_3$): 3.69 (t,12.6Hz,8H),-CH_2O; 2.87(s,br,8H),SCH_2CH_2S; 2.75(t,12.6Hz,8H). ^{13}C NMR($CDCl_3$): 71.9,-CH_2O; 32.5,SCH_2-; 31.1,$(CH_2S)_2$. High resolution mass spectral data: Calcd for $C_{12}H_{24}O_2S_4$: m/e 328.0658(M$^+$); found: m/e 328.0653(M$^+$). Anal. calcd. for $C_{12}H_{24}O_2S_4$: C 43.87, H 7.38; found: C 43.94, H 7.31.

2.2.2. X-ray Crystallography

A colourless irregular crystal of [18]aneO_2S_4 having approximate dimensions of 0.400×0.300×0.200 mm was mounted on a glass fibre. All measurements were made on a Rigaku AFC6S diffractometer with graphite monochromated Mo Kα radiation and a 2KW sealed tube generator. Crystallographic data are summarized in table 2-1.

Table 2-1. Crystal Data for [18]aneO_2S_4

chem formula	$C_{12}H_{24}O_2S_4$	V(Å^3)	398.0(2)
fw	328.56	Z	1
space group	P1(No.2)	ρ_{calcd}(g cm^{-1})	1.371
a(Å)	7.204(1)	μ(cm^{-1})	5.66
b(Å)	10.770(2)	λ(Å)	0.71069
c(Å)	5.262(2)	R	0.024
α(deg)	99.35(2)	R_w	0.022
β(deg)	92.18(2)	T(°C)	26
γ(deg)	98.08(1)		

$$R = \sum ||Fo| - |Fc|| \; / \sum |Fo|$$

$$R_w = [(\sum w (||Fo| - |Fc||)^2 / \sum w Fo^2)]^{1/2}$$

2.3. Results and Discussion

2.3.1. Synthesis

Bradshaw and coworkers reported the preparation of [9]aneOS$_2$ and [18]aneO$_2$S$_4$ by the reaction of bis-(2-chloroethyl)ether with 1,2-ethanedithiol in ethanol under the presence of sodium hydroxide [10]. Their yields obtained for [9]aneOS$_2$ and [18]aneO$_2$S$_4$ were 6% and 4%, respectively, which are much less than the yields reported herein.

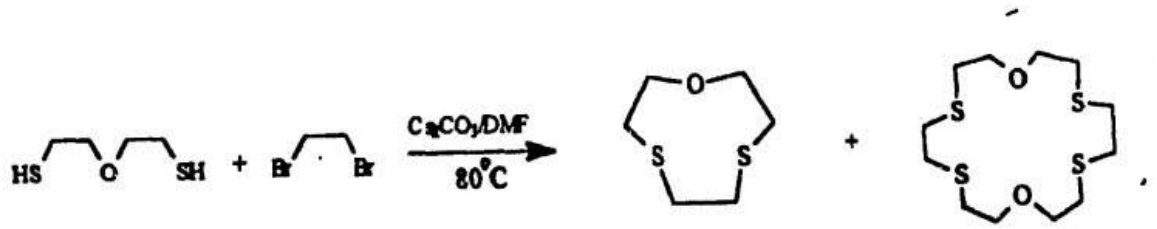

The use of cesium carbonate, as we expected, improved the cyclization yield greatly. This "cesium effect" has been discussed in chapter I. The yield depends critically upon the rate of addition and temperature. Faster rates and lower temperatures will reduce the yield.

[9]aneOS$_2$ is soluble in dichloromethane, diethyl ether, ethanol, and insoluble in water. [18]aneO$_2$S$_4$ is soluble in dichloromethane, benzene, and hot ethanol, and is insoluble in water.

2.3.2. Conformation studies of [9]aneOS$_2$

Conformation studies of medium to large macrocyclic thioethers (≥12 ring atoms) indicate that in the solid state, in the absence of other structural constraints, most of these ligands adopt an exo conformation with the sulfur atom pointing out of the macrocyclic cavity. Cooper and coworkers explained this phenomenon as a consequence of the tendency of the C-S-C-C linkages to adopt a gauche conformation [11]. A maximum number of such gauche arrangements is obtained when the sulfur atoms have positions in the "corners" of the macrocycle. This is in contrast with what is observed for the analogous crown oxyethers, in which the C-O-C-C linkages prefer anti placements, and oxygen atoms are often found on the "sides" of the macrocycle [11,16].

When ring sizes become smaller (≤ 11 ring atoms), however, flexibility of the rings becomes less and structural constraints take effect. One would also expect 1,4 and 1,5 interactions across the ring to be significant in determining the conformation of the ring.

The single-crystal X-ray structure of metal-free [9]aneS$_3$ [17] shows it to adopt a [333] endo conformation with C_3 symmetry [18]. Molecular mechanics calculations, however, indicate the [1222] conformations of C_1 and C_2 symmetry are more stable, and these calculation results are supported by electron diffraction

experiments [19-21]. Usually there are some effects such as crystal-packing forces which select a particular conformation during crystallization, even if it is present as a minor component of a mixture of the conformers.

It would be interesting to determine the conformation of [9]aneOS$_2$ because it is a small mixed-donor ligand. The conformation of [9]aneOS$_2$ should present a balance of preferences for both S atoms and O atoms in a small ring. Unfortunately, we were not able to obtain its crystal structure because [9]aneOS$_2$ is liquid. We report here the results of molecular-mechanics calculations (MM3) on [9]aneOS$_2$ as a free ligand [22].

Conformation I - The calculations indicate that this conformation has lowest strain energy (85.82 kJ/mol), as shown in Fig. 2-1. This model is similar to Dale's [1222] conformation [13,18], and the [1222] conformation is found with the global minimum energy in [9]aneS$_3$, too [19,21]. The two sulfur atoms take up exo positions and oxygen atom is in an endo orientation. The S-C-C-S linkage adopts anti placement, which reduces the repulsive force between two S atoms. However, the different orientations of S atoms, with respect to a mean plane defined by the ring, make them unsuitable to chelate metal atoms, and one would expect that this conformation only exists in the free ligand and can rarely be found in the metal complexes of [9]aneOS$_2$.

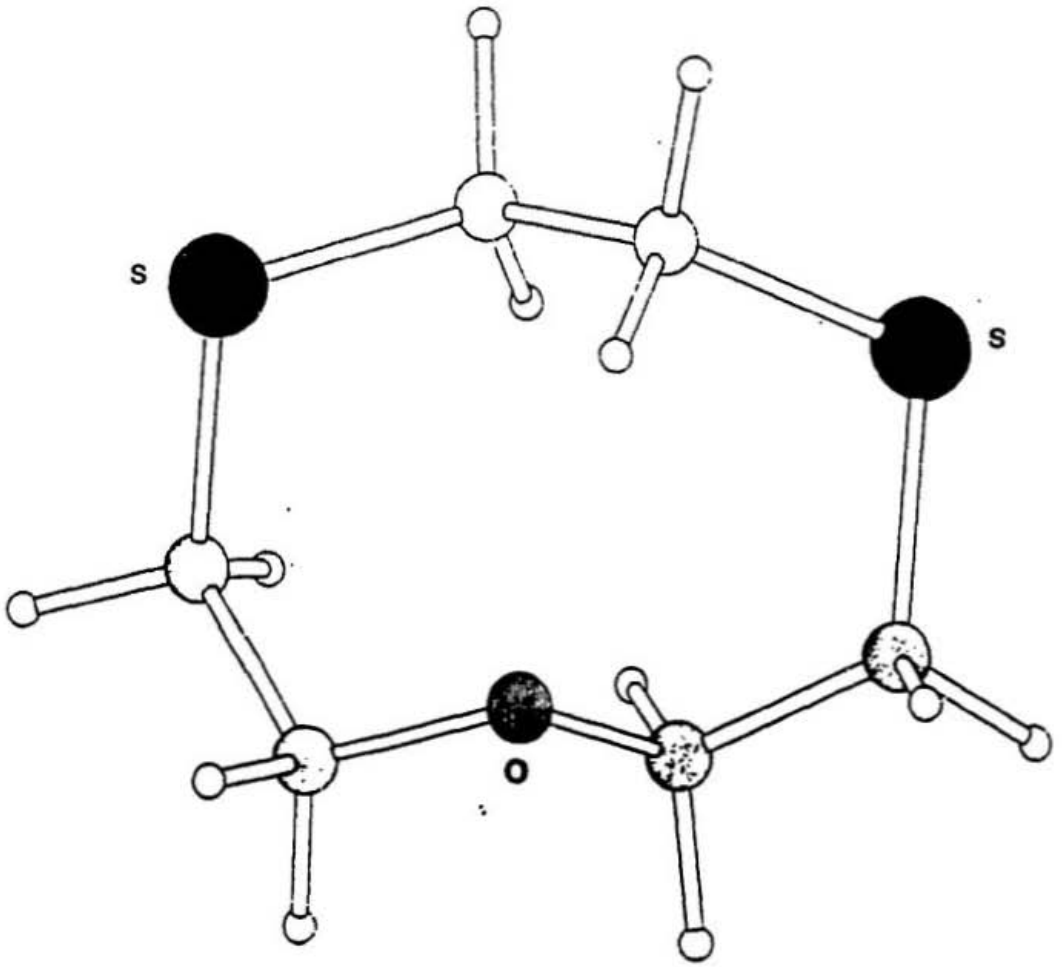

Fig. 2-1 Conformation I of [9]aneOS$_2$

Conformation II - This model is illustrated in Fig. 2-2, and is similar to Dale's [234] conformation. The S-C-C-S linkage has gauche placement, and the C-O-C-C group adopts anti placement. The three hetero-atoms have a down-down-up (anti) conformation. The MM3 calculation indicates conformation II has the second lowest strain energy and is less stable than conformation I by only 0.950 kJ/mol. Thus, [9]aneOS$_2$ is able to chelate a metal atom through its two sulfur atoms with little rearrangement by this conformation.

The energetic difference between conformation I and II derives mainly from the possible 1,5 O···H interaction. Such 1,5 interactions were invoked to account for the conformation of [9]aneO$_3$, which has been shown to adopt a [234] conformation [23,24], but S···H contacts would not be expected to be so significant energetically as O···H interactions.

Conformation III - This conformation (Fig. 2-3) is Dale's [333] conformation and permits [9]aneOS$_2$ to adopt facial coordination to metal atoms as does [9]aneS$_3$. The calculations show that conformation III is a little less stable with strain energy equal to 91.977 kJ/mol. Therefore, conformational rearrangement is required for [9]aneOS$_2$ to act as a tridentate ligand, but not for [9]aneS$_3$ which is pre-organized for facial coordination [20].

In summary, the calculations show that conformation I is the most stable for metal-free [9]aneOS$_2$. However, if [9]aneOS$_2$

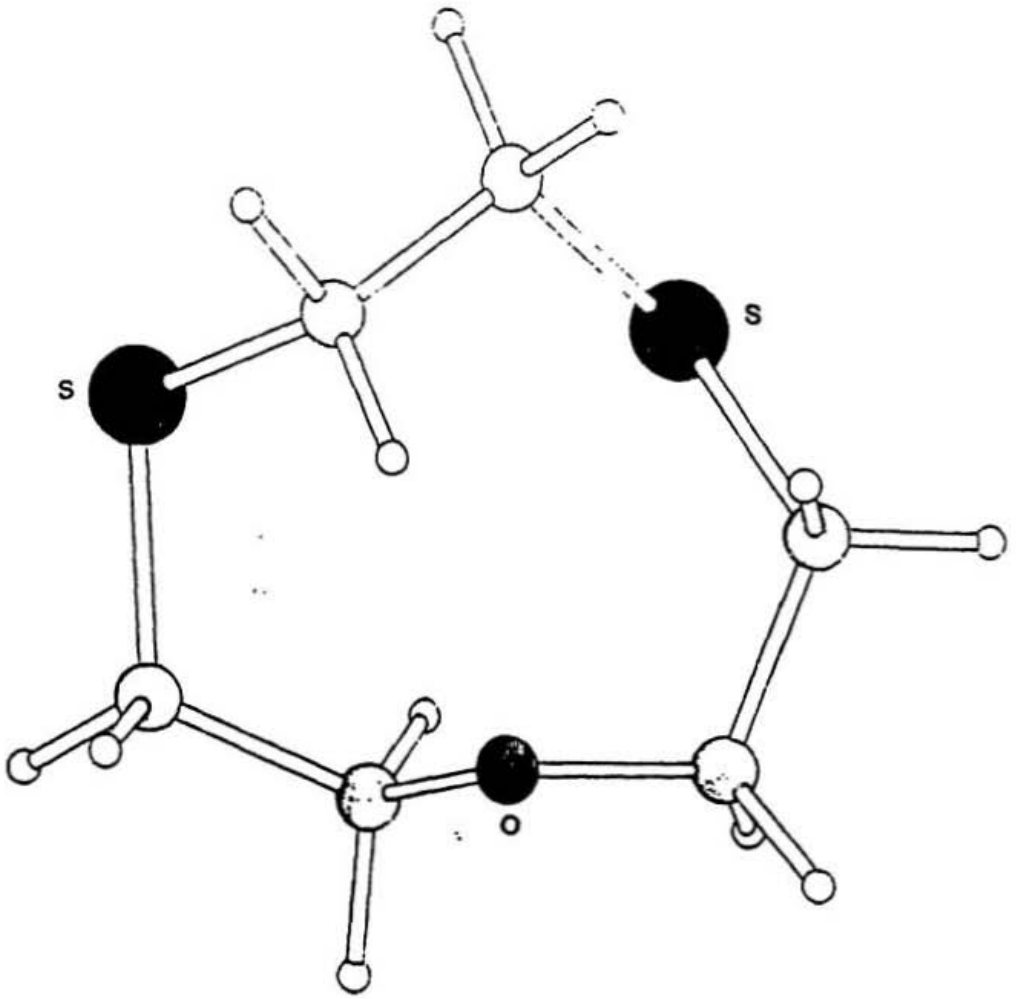

Fig. 2-2 Conformation II of [9]aneOS$_2$

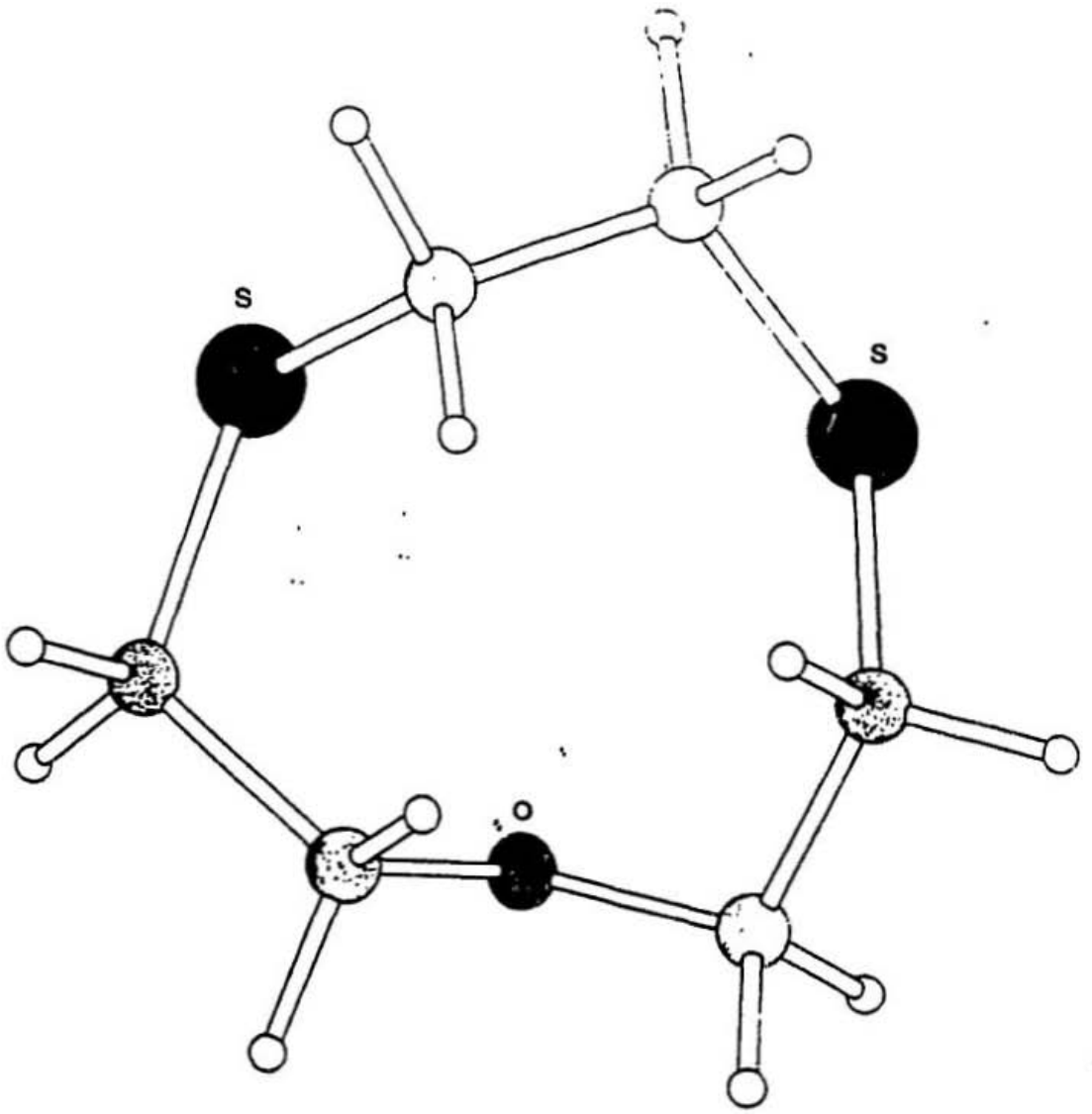

Fig. 2-3 Conformation II of [9]aneOS$_2$

chelates a metal atom as a bidentate ligand, conformation **II** ([234] mode) is the most likely one which [9]aneOS$_2$ adopts in its metal complexes. In contrast to this, the [333] conformation of [9]aneS$_3$ dominates its complexes [25]. The difference mainly stems from the different conformational preferences of S and O donors.

Finally we should point out that MM3 calculations do not allow us to reach an unequivocal conclusion about the conformation present. As we see, the strain energies of the conformers do not differ enormously. Nevertheless, these calculations do give us information about values of the various structural parameters of the different conformers, as well as giving an indication of the relative stability (and hence abundance) of various conformers.

2.3.3. X-ray structure and conformation of [18]aneO$_2$S$_4$

The unit cell contains one molecule of [18]aneO$_2$S$_4$. An ORTEP perspective view of the molecule, indicating the atom-numbering scheme, is shown in Figure 2-4. Selected bond distances and angles are listed in Table 2-2. Carbon-sulfur bond lengths range from 1.807(2) Å to 1.817(2) Å and agree with those found in hexathia-18-crown-6 ([18]aneS$_6$) and trithia-9-crown-3 ([9]aneS$_3$). As in the other cyclic structures, the C-C bonds in [18]aneO$_2$S$_4$ (1.418(2) Å to 1.503(3) Å) are significantly shorter

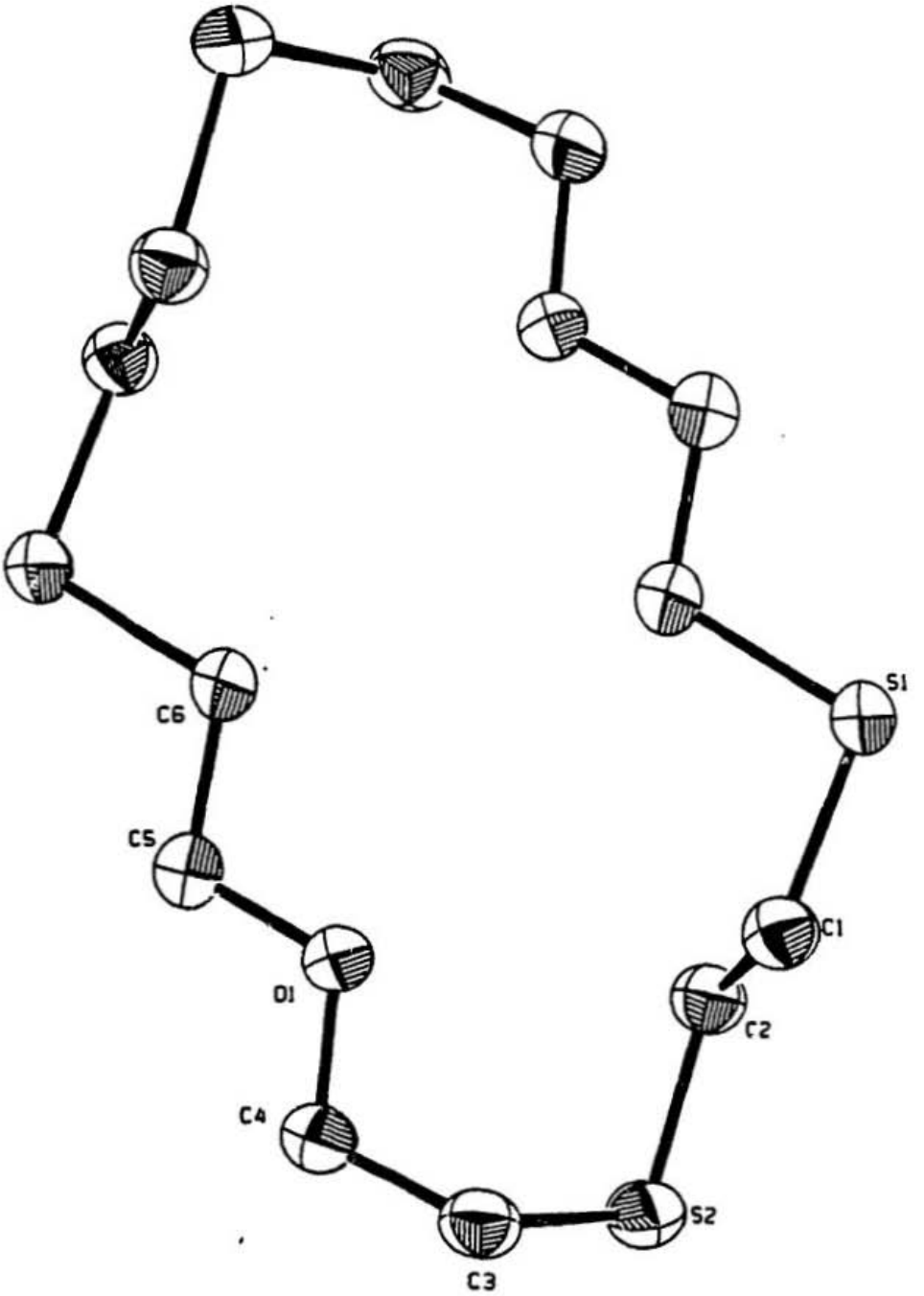

Fig. 2-4 The stucture of [18]aneO_2S_4

than the value expected for $C(sp^3)$-$C(sp^3)$ linkages (1.54 Å) [11]. They compare well, however, with those for other crown ethers such as, for example, [18]aneO_4S_2 and [12]aneOS_3 [14,15].

Table 2-2. Selected Geometrical Parameters of [18]aneO_2S_4

Intramolecular Distances (Å)					
atom	atom	distance	atom	atom	distance
S(1)	C(1)	1.813(2)	O(1)	C(5)	1.418(2)
S(1)	C(6)	1.809(2)	C(1)	C(2)	1.503(3)
S(2)	C(2)	1.817(2)	C(3)	C(4)	1.499(3)
S(2)	C(3)	1.807(2)	C(5)	C(6)	1.501(2)
O(1)	C(4)	1.419(2)			

Intramolecular Bond Angles (deg.)							
atom	atom	atom	angle	atom	atom	atom	angle
C(1)	S(1)	C(6)	100.07(9)	S(2)	C(3)	C(4)	116.9(1)
C(2)	S(2)	C(3)	104.61(9)	O(1)	C(4)	C(3)	109.2(1)
C(4)	O(1)	C(5)	112.6(1)	O(1)	C(5)	C(6)	107.4(1)
S(1)	C(1)	C(2)	113.5(1)	S(1)	C(6)	C(5)	109.7(1)
S(2)	C(2)	C(1)	113.7(1)				

Table 2-3. Torsion Angles for [18]aneO_2S_4 (deg.)

atoms	angle	atoms	angle
S(1) C(1) C(2) S(2)	174.5(1)	C(2) S(2) C(3) C(4)	71.0(2)
S(1) C(6) C(5) O(1)	178.6(1)	C(2) C(1) S(1) C(6)	69.3(2)
S(2) C(3) C(4) O(1)	-73.3(2)	C(3) C(4) O(1) C(5)	-174.0(2)
C(1) S(1) C(6) C(5)	174.5(1)	C(4) O(1) C(5) C(6)	-179.3(2)
C(1) C(2) S(2) C(3)	62.1(2)		

The molecule is centrosymmetric as shown in Fig. 2-4. The conformational preferences of both S atoms and O atoms manifest themselves clearly in this mixed oxa-thia macrocycle. All four sulfur atoms are exodentate, and two oxygen atoms are endodentate. Of interest is the fact that hexathia-18-crown-6 has four exodentate and two endodentate donors, too [11]. The torsion angles are presented in Table 3-3. In accord with the predictions of Cooper and coworkers [11], six of eight C-S-C-C linkages adopt gauche placements, while in contrast, all four C-O-C-C units adopt anti arrangements.

2.4. References

1. Cooper, S.R.; Rawle, S.C., Struct. Bonding, *72*, 1 (1990).
2. Blake, A.J.; Schröder, M., Adv. Inorg. Chem., *35*, 2 (1990).
3. Blake, A.J.; Holder, A.J.; Hyde, T.I.; Roberts, Y.V.; Lavery, A.J.; Schröder, M., J. Organomet. Chem., *323*, 261 (1987).
4. Blake, A.J.; Gould, R.O.; Holder, A.J.; Hyde, T.I.; Lavery, A.J.; Odulate, M.O.; Schröder, M., J. Chem. Soc., Chem. Commun., 118 (1987).
5. Clarkson, J.; Yagbasan, R.; Blower, P.J.; Rawle, S.C.; Cooper, S.R., J. Chem. Soc., Chem. Commun., 950 (1987).
6. Blake, A.J.; Crofts, R.D.; Groot, B.; Schröder, M., J. Chem. Soc., Dalton Trans., 485 (1993).
7. McAuley, A.; Subramanian, S., Inorg. Chem., *29*, 2830 (1990).
8. Hancock, R.D.; Dobson, S.M.; Boeyenes, C.J.A., Inorg. Chim. Acta, *133*, 221 (1987).
9. Spiro,, T.G., Copper Proteins, A Wiley-Interscience Publication, NY, P122 (1981).
10. Bradshaw, J.S.; Hui, J.Y.; Haymore, B.L.; Christensen, J.J.; Izatt, R.M., J. Heterocyclic Chem., *10*, 1 (1973).
11. Wolf, R.E.; Hartman, J.R.; Storey, J.M.E.; Foxman, B.M.; Cooper, S.R., J. Am. Chem. Soc., *109*, 4328 (1987).
12. Glass, R.S.; Wilson, G.S.; Setzer, W.N.; J. Am. Chem.

Soc., *102*, 5068 (1980).

13. Dale, J., Acta Chem. Scand., *27*, 1115 (1973).
14. Dalley, N.K.; Smith, J.S.; Larson, S.B.; Matheson, K.L.; Izatt, R.M.; Christensen, J.J., J. Heterocycl. Chem., *18*, 463 (1981).
15. Bradshaw, J.S.; Hui, J.Y.; Chan, Y.; Haymore, B.L.; Izatt, R.M.; Christensen, J.J., J. Heterocycl. Chem., *11*, 47 (1974).
16. DeSimone, R.E.; Glick, M.D., J. Am. Chem. Soc., *98*, 762 (1976).
17. Glass, R.S.; Wilson, G.S.; and Setzer, W.N., J. Am. Chem. Soc., 102, 5068 (1980).
18. Boeyens, J.C.A; Dobson, S.M., Stereochemical and Stereophysical Behaviour of Macrocycles, Bernal, I., Ed., Elsevier Science Publishing Company Inc., New York, NY, P2-102 (1987).
19. Blom, R.; Rankin, D.W.H.; Robertson, H.E.; Schröder, M.; Taylor, A., J. Chem. Soc., Perkin Trans., 2, 773 (1991).
20. Durrant, M.C.; Richards, R.L.; Firth, S.; J. Chem. Soc., Perkin Trans., 2, 445 (1993).
21. Setzer, W.N.; Coleman, B.R.; Wilson, G.S.; Glass, R.S., Tetrahedron, *17*, 2743 (1981).
22. Molecular mechanics calculations (MM3) were performed by Dr. T.B. Grindley, Dalhousie University.
23. Borgen, G.; Dale, J.; Anet, F.A.L.; Krane, J., J. Chem.

Soc., Chem. Commun., 243 (1974).

24. Dale, J., Isr. J. Chem., *20*, 3(1980).

III. Synthesis and Properties of [Pd([9]aneOS$_2$)Cl$_2$] and [Pt([9]aneOS$_2$)Cl$_2$]

3.1. Introduction

Since the first recognition of a stereochemically non-rigid sulfur chelate complex [$PtCl_2(MeSCH_2CH_2SMe)$] was reported in 1966 [25], widespread fluxionality in sulfur and selenium complexes has been discovered [11,13]. For complexes of macrocyclic thioethers, however, few examples of stereochemical nonrigidity have been reported [15,20] probably as a consequence of the conformational constraints of the ligand. We report herein the first example of fluxionality involving the oxygen atom in a macrocyclic thioether-ether ligand. The coordination properties of thioether complexes are currently of considerable interest in several areas, not the least of which involve studies of catalytic hydrodesulfurization [26] and of cellular sulfur donor reactions with platinum anticancer drugs [27].

3.2. Experimental Section

3.2.1. Preparation of [Pd([9]aneOS$_2$)Cl$_2$]

A solution of [9]aneOS$_2$ (112 mg, 0.683 mmol) in 10 mL of acetonitrile was added to a solution of cis-$PdCl_2(PhCN)_2$ (230 mg, 0.600 mmol) in 20 mL of acetonitrile to give an orange solution,

which immediately precipitated an orange solid. The precipitate was filtered, washed with acetonitrile and diethyl ether, and dried in vacuum. Yield 180 mg (88%). IR (cm^{-1}, KBr, Nujol): 2923(vs), 2855(vs), 1488(s), 1464(s), 1378(s), 1299(s), 1124(s), 1055(m), 1018(s), 920(m), 805(w), 722(w), 663(w), 611(w), 508(w). Anal. calcd. for $C_6H_{12}Cl_2OPdS_2$: C 21.10, H 3.54; found: C 21.20, H 3.60.

3.2.2. Preparation of [Pt([9]OS_2)Cl_2]

K_2PtCl_4 (125 mg, 0.300 mmol) was treated with [9]aneOS_2 (55.7 mg, 0.340 mmol) in refluxing acetonitrile (50 mL) for 12 h under N_2. The yellow precipitate that formed was filtered and washed with water, acetonitrile and diethyl ether, and then dried in vacuum. Yield 106 mg (79%). IR (cm^{-1}, KBr, Nujol): 2923(vs), 2854(vs), 1461(s), 1377(m), 1281(w), 1229(w), 1127(s), 1056(w), 1019(m), 917(w), 722(w).

3.2.3. X-ray Crystallography

Red orange crystals of [Pd([9]aneOS_2)Cl_2] were obtained by vapour diffusion of diethyl ether into a solution of the complex in dimethyl sulfoxide. All measurements were made on a Rigaku AFC6S diffractometer with graphite monochromated Mo Kα radiation and a 2KW sealed tube generator. The crystallographic data are

listed in Table 3-1.

Table 3-1. Crystal Data for [Pd([9]aneOS$_2$)Cl$_2$]

chem formula	$C_6H_{12}Cl_2OPdS_2$	V(Å^3)	1035.2(1)
fw	341.59	Z	4
space group	$P2_1/n$(No.14)	ρ_{calcd}(g cm^{-1})	2.192
a(Å)	8.464(2)	μ(cm^{-1})	26.32
b(Å)	12.199(2)	λ(Å)	0.71069
c(Å)	10.384(2)	R	0.024
β(deg)	105.09(1)	R_w	0.033
T(°C)	26		

3.3. Results and Discussion

3.3.1. Description of Structure

A PLUTO plot of [Pd([9]aneOS$_2$)Cl$_2$] is shown in Fig. 3-1. The bond distances and angles are listed in Table 3-2.

The [9]aneOS$_2$ assumes a facial coordination mode on Pd(II). The central Pd atom lies 0.0111 Å above the mean square plane consisting of two chloride ligands (Pd-Cl1 = 2.331(1), Pd-Cl2 = 2.333(1) Å) and two adjacent sulfur atoms (Pd-S1 = 2.268(1), Pd-S2 = 2.258(1) Å). These values compare well with those Pd-S (2.245-2.282 Å) and Pd-Cl (2.3316-2.3326 Å) [1] bond distances

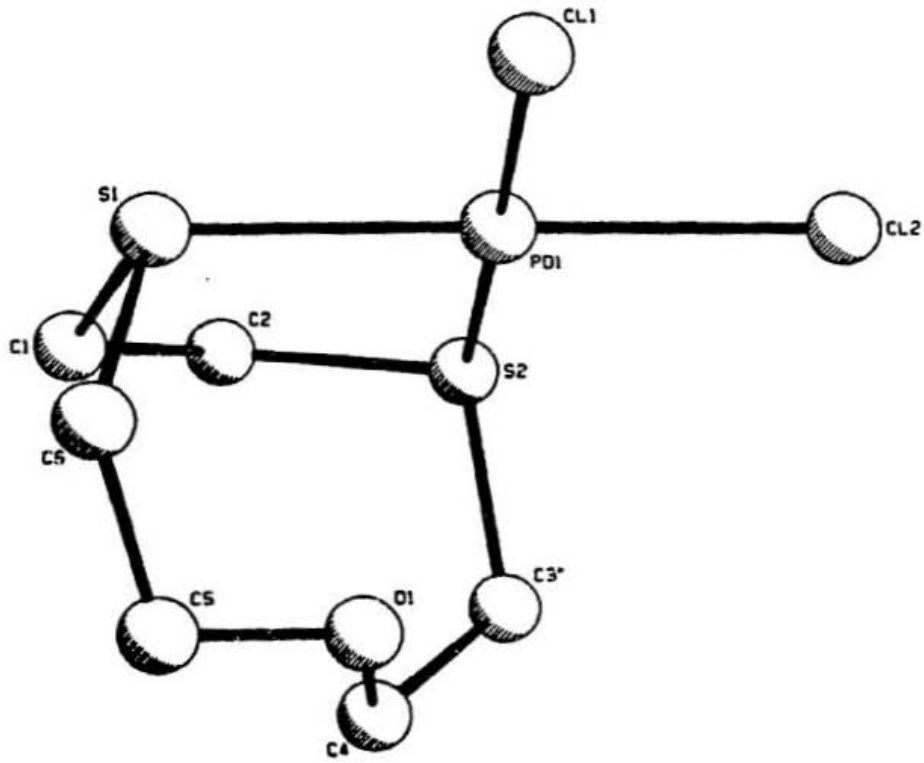

Fig. 3-1 The structure of $[Pd([9]aneOS_2)Cl_2]$

Table 3-2. Selected Bond Lengths and Angles in [Pd([9]aneOS$_2$)Cl$_2$]

Distances (Å)

atom	atom	distance	atom	atom	distance
Pd(1)	Cl(1)	2.331(1)	S(2)	C(3)	1.817(5)
Pd(1)	Cl(2)	2.333(1)	O(1)	C(4)	1.421(5)
Pd(1)	S(1)	2.268(1)	O(1)	C(5)	1.422(5)
Pd(1)	S(2)	2.258(1)	C(1)	C(2)	1.518(6)
S(1)	C(1)	1.839(4)	C(3)	C(4)	1.505(6)
S(1)	C(6)	1.823(4)	C(5)	C(6)	1.510(6)
S(2)	C(2)	1.816(4)			

Bond Angles (deg.)

atom	atom	atom	angle	atom	atom	atom	angle
Cl(1)	Pd(1)	Cl(2)	93.12(4)	Pd(1)	S(2)	C(3)	105.9(2)
Cl(1)	Pd(1)	S(1)	88.14(4)	C(2)	S(2)	C(3)	104.7(2)
Cl(1)	Pd(1)	S(2)	177.93(4)	C(4)	O(1)	C(5)	116.7(3)
Cl(2)	Pd(1)	S(1)	178.74(4)	S(1)	C(1)	C(2)	114.1(3)
Cl(2)	Pd(1)	S(2)	88.52(4)	S(2)	C(2)	C(1)	116.4(3)
S(1)	Pd(1)	S(2)	90.23(4)	S(2)	C(3)	C(4)	117.9(3)

found in other Pd[II] complexes of macrocyclic thioethers [1,27-28].

The oxygen atom is oriented toward the palladium centre above the square coordination plane with an unusually long Pd-O distance (Pd-O = 2.968(3) Å), although similar types of Pd-O interactions have been observed in other Pd(II) complexes. When the apex of the pyramid is occupied by an oxygen atom, in general the Pd-O bond lengths are significantly longer than those in equatorial positions. For example, the axial Pd-O bond distance in [Pd([15]aneN$_2$OS$_2$] is 2.779(4) Å [31], and for [Pd(hfac)$_2${P(o-tolyl)$_3$}] [29] and [Pd(hfac)(triphos)] [30] it is 2.797(6) Å and 2.653(6) Å respectively. In contrast, the Pd-O bond length in equatorial site is 2.110(3) Å for [Pd(F$_6$acac)$_2$(triphos)]$^+$ [32] and 1.98 Å (average length) for the square planar cis-[{Pd{PhC(O)CHC(O)Me}$_2$] [33,34]. Though the apical Pd-O bond distance found in [Pd([9]aneOS$_2$)Cl$_2$] is longer than those values reported for Pd(II) complexes, there is no reason to exclude a subtle Pd-O interaction. In fact, this distance is significantly less than the sum of the van der Waals' radii (3.10 Å) of Pd and O atoms [36], and the existence of a Pd-O bond is supported by NMR studies (vide infra). Thus, the structure of [Pd([9]aneOS$_2$)Cl$_2$] is better considered as an intermediate between square-planar and square pyramidal geometry.

It is notable that the unusual [234] ring conformation is

found in Pd([9]aneOS$_2$)Cl$_2$ (torsion angles are presented in Table 3-3), whereas the [333] conformation dominates all other [9]aneX$_3$ (X = N,S) complexes [5]. For all S-N mixed donor [9]aneX$_3$ ligands

Table 3-3. Ligand Torsion Angles in [Pd([9]aneOS$_2$)Cl$_2$]

atoms	angle	atoms	angle
S(1) C(1) C(2) S(2)	31.8(5)	S(1) C(6) C(5) O(1)	45.6(5)
S(2) C(3) C(4) O(1)	-52.6(5)	C(1) S(1) C(6) C(5)	43.9(4)
C(1) C(2) S(2) C(3)	81.7(4)	C(2) S(2) C(3) C(4)	-51.0(4)
C(2) C(1) S(1) C(6)	-126.3(3)	C(3) C(4) O(1) C(5)	143.1(4)
C(4) O(1) C(5) C(6)	-130.0(4)		

in their free forms, molecular mechanics simulation indicates that the [234] configurations are more strained than the [333] forms by about 12-20 kJ mol^{-1} [5,6]. The same difference is found in metal complexes [5,6]. For [9]aneOS$_2$, however, the [333] conformation is less stable than the [234] form (see Chapt. III) due to different conformation preferences around sulfur and oxygen atoms. Thus, in [Pd([9]aneOS$_2$)Cl$_2$] the [9]aneOS$_2$ ring adopts the [234] conformation. Furthermore, this [234] conformation allows the oxygen donor in Pd([9]aneOS$_2$)Cl$_2$ to

occupy the axial coordination site and form square-pyramidal geometry.

3.3.2.Electronic Spectra

The electronic spectrum of Pd([9]aneOS$_2$)Cl$_2$ in dichloromethane exhibits two main bands - at 250 nm (ε = 7300 M^{-1} cm^{-1}) with 277 nm(sh), and at 406 nm (ε = 716 M^{-1} cm^{-1}). These absorptions represent the characteristic electronic spectra of square-planar Pd(II) complexes [2]. The band at 250 nm is due to a charge transfer from the chloride ligands to the Pd d_{x2-y2} orbital, while the absorption at 277 nm belongs to a charge transfer from the sulfur bonding orbitals to Pd d_{x2-y2}. The weaker band at 406 nm is d-d transfer in nature [3,4].

3.3.2. Variable Temperature NMR studies

The complex is quite soluble in DMSO but less soluble in other solvents, such as nitromethane and dichloromethane.

The ^1H spectra recorded in d_5-nitrobenzene at room temperature are shown in Fig. 3-2. The complicated spectrum is in accord with the rigid structure illustrated in Fig. 3-1, which results in non-equivalent protons in the ^1H NMR for each of the 12 hydrogen atoms in the macrocyclic ring. These hydrogen atoms present three AB patterns of which two are overlapping.

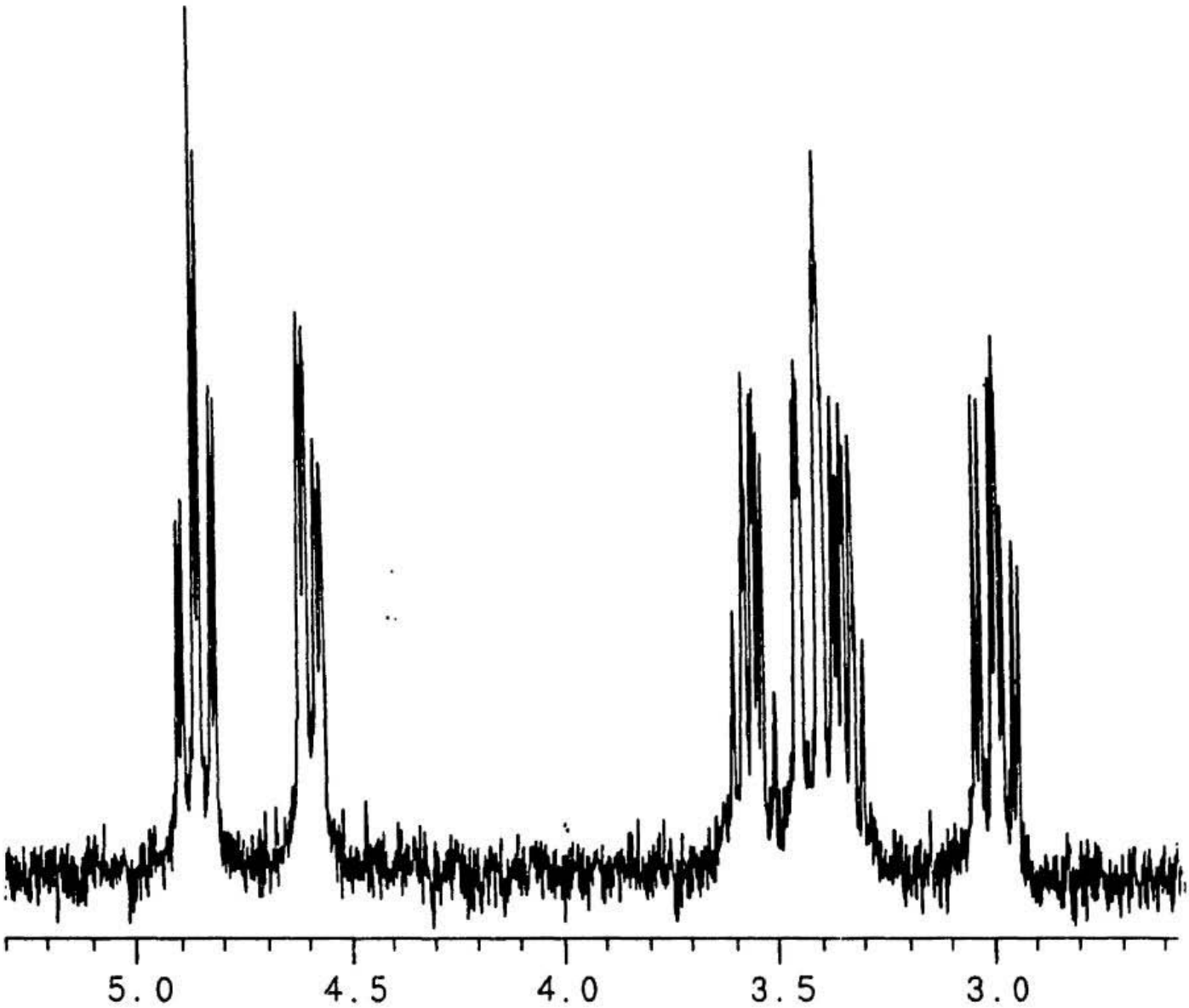

Fig. 3-2. ^1H NMR spectrum of [Pd([9]aneOS$_2$)Cl$_2$] in d_5-nitrobenzene at 22°C

The two resonances in the range 4.61-4.91 ppm are caused by the four protons in the $-CH_2OCH_2-$ group, which occur at a much lower field compared with those of the free ligand (3.95 ppm). Two of the four protons in the $-SCH_2CH_2S-$ region resonate in the 3.56-3.66 ppm range, while the other two proton signals overlap with the two hydrogen atoms coming from the $-CH_2S-$ group to give the multiple resonances in the area of 3.39-3.49 ppm. The high field multiple signals at 3.00-3.10 ppm are assigned to the two H atoms in the $-CH_2S-$ group. Raising the temperature to 140°C results in no change in the ^1H NMR spectra in this solvent.

Since the analysis (above) of this spectrum is consistent with the solid state structure revealed by X-ray crystallography, it would appear that the structure of $[Pd([9]aneOS_2)Cl_2]$ in solution remains the same as it is in the solid state.

When dimethyl sulfoxide (DMSO) is used as the solvent, the situation is different (Fig. 3-3). On raising the temperature of the solution from 22°C to 120°C, the two $-CH_2O-$ signals coalesce to a single broad band, and the multiple peaks in the $-SCH_2CH_2S-$ and $-CH_2S-$ regions also merge into two other broad resonances. The different observations in nitrobenzene and dimethyl sulfoxide solutions indicate a solvent-involved fluxional process. At least four possible mechanisms can explain such an averaging process. These include:

(1) a synchronous or correlated inversion of all three

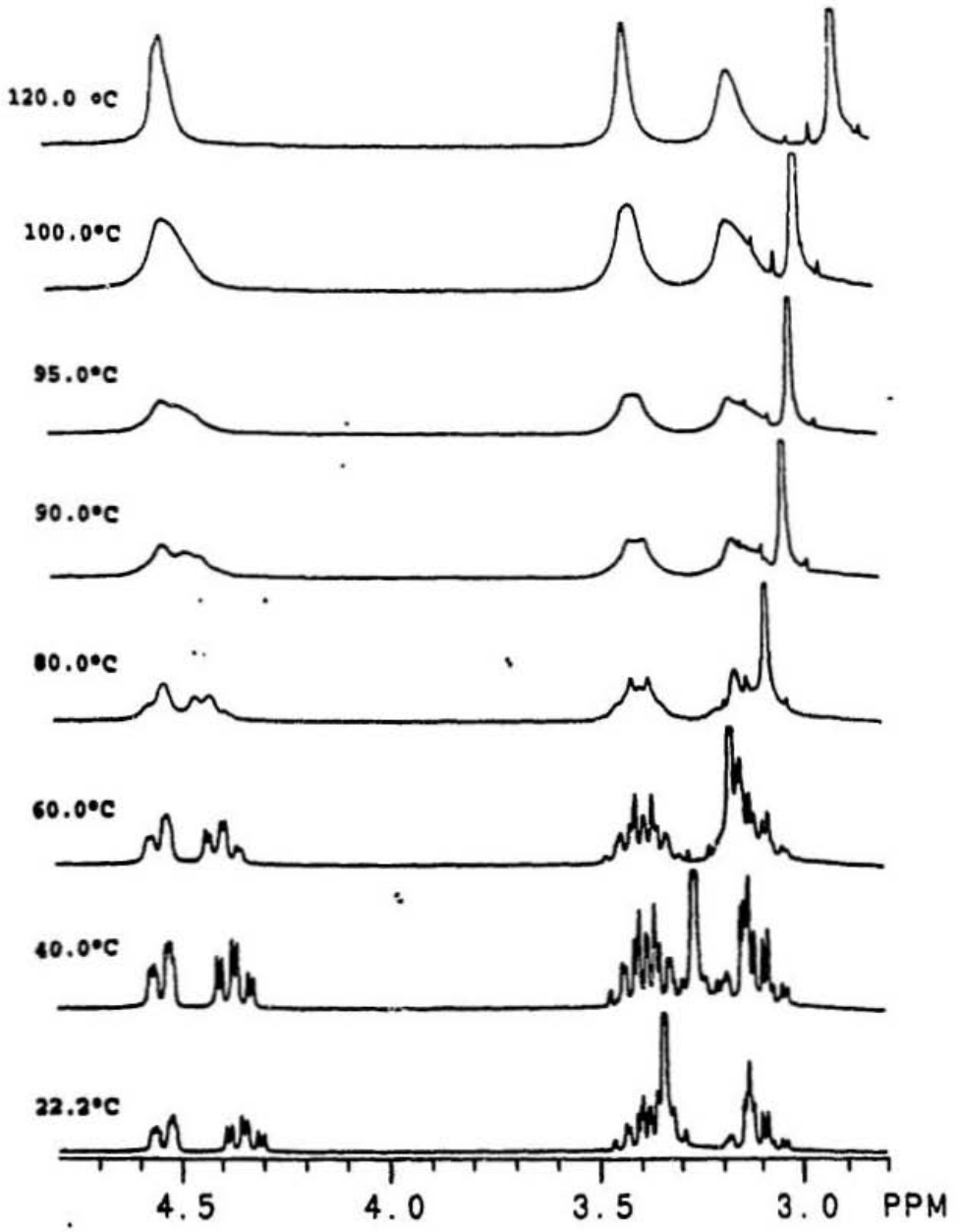

Fig. 3-3. The variable-temperature ^1H NMR spectra of [Pd([9]aneOS$_2$)Cl$_2$] in d$_6$-DMSO solution from 22°C to 120°C

coordinated atoms.

(2) a Berry pseudo-rotation process.

(3) a process that permutes the three coordination sites of the macrocyclic ring over the palladium dichloride moiety.

(4) a dissociation-recombination of ligand

Process (1) can be ruled out, since in such small ring, when three hetero-atoms bind to the central metal, the highly strained structure prevents overall inversion, even though the inversion process is often observed in open chain ligand complexes [7-9] at ambient temperature and involves a low energy barrier ($\Delta G^{\neq}$ = 40-70 kJ mol^{-1}) [10,11].

Process 2, on the other hand, seems a plausible route due to a widespread observation of this kind of stereochemical non-rigidity in five-coordinated complexes [21-23,35]. This process would involve a concerted axial-equatorial bond-bending motion that allows the interconversion between square pyramidal geometry and trigonal bipyramidal geometry along a low energy pathway [12], as illustrated in Scheme 3-1.

Scheme 3-1. Berry Pseudorotation

from temperature-dependent ^1H NMR spectral data and indicates intramolecular ligands exchange in the fluxional process [13,14]. In other words, Berry pseudorotation involves a non-dissociative pathway.

In order to distiguish whether the fluxion in [Pd([9]aneOS$_2$)Cl$_2$] proceeds by a dissociative or non-dissociative mechanism, we added free [9]aneOS$_2$ ligand to the d_6-DMSO solution of the Pd complex. The variable-temperature ^1H NMR of this solution is shown in Fig. 3-4. When the solution was warmed, the three ligand resonances (at 2.79, 3.07, and 3.94 ppm) began to diminish. As the temperature continued to rise, the free ligand signals continue to broaden until at 140°C they have almost disappeared, and at the same time the resonances of Pd([9]aneOS$_2$)Cl$_2$ became much broadened. The observations unequivocally indicate the presence of a ligand-exchange process. Thus, the fluxional rearrangement involves a dissociative mechanism that excludes pathway (2).

The fluxionality which averages the methylene protons can also be achieved by a rotation process of the macrocyclic ligand - process (3). Abel and coworkers first reported rotational fluxion of crown thioether ligand which proceeds via a series of correlated 1,4-metallotropic shifts (Scheme 3-2) [15], and similar observations have been reported recently in a series of [9]aneS$_3$ complexes: PtRR'([9]aneS$_3$) [R = R' = Me, Et, CH_2CME_3,

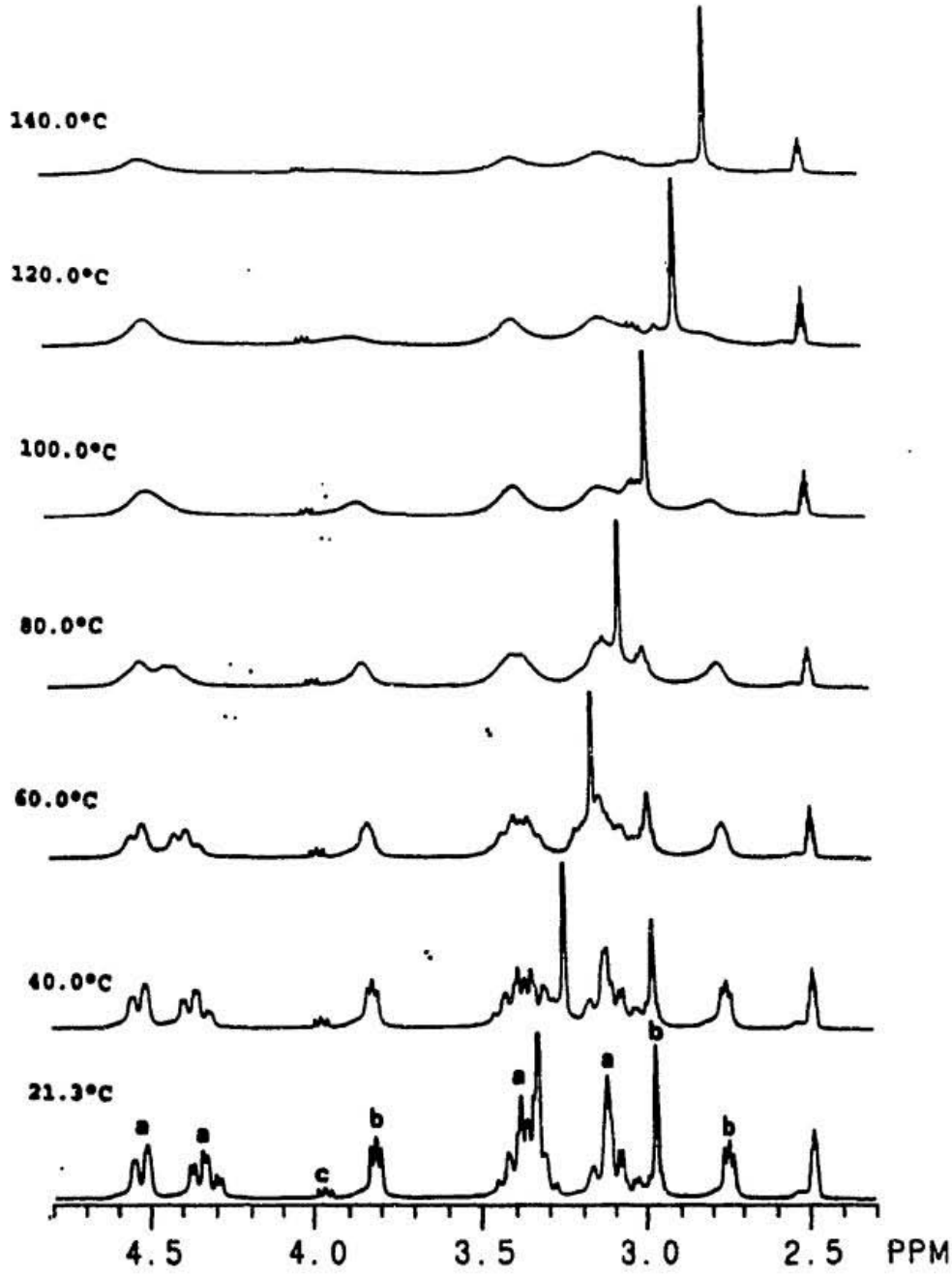

Fig.3-4 Variable-temperature ^1H NMR spectra of [Pd([9]aneOS$_2$)Cl$_2$] in d_6-DMSO with free ligand [9]aneOS$_2$. (a) complex (b) free ligand (c) impurity in the free ligand.

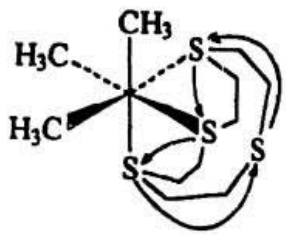

Scheme 3-2

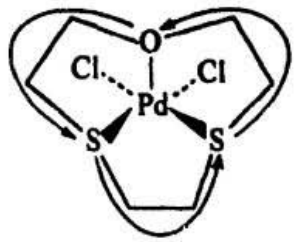

Scheme 3-3

CH_2SiMe_3 Ph; R = Me, R' = CH_2SiMe_3; R = Cl, R' = CH_2SiMe_3] [20]. The fluxional process of [Pd([9]aneOS$_2$)Cl$_2$], however, is unlikely to involve the 1,4-shift mechanism. First of all, the 1,4-metallotropic shift was believed to be a intramolecular process [15,20], while the fluxional rearrangement in [Pd([9]aneOS$_2$)Cl$_2$] proceeds *via* a dissociative pathway. Second, if [Pd([9]aneOS$_2$)Cl$_2$] undergoes a similar 1,4-shift, the oxygen donor occupying the apical position will move to the equatorial position, and at the same time, one of the two equatorial sulfur donors will move to the axial position, as shown in Scheme 3-3. However, this kind of shift is not in accord with the spectral changes observed. In Fig. 3-3, the three types of methylene protons resonate at essentially constant chemical shifts throughout the temperature change from 22°C to 120°C. This indicates there is no apical-equatorial donor changes in the fluxional process, because, otherwise, the ^{1}H resonances should shift. Furthermore, variable-temperature ^{13}C NMR results also

Table 3-4. Variable-temperature ^{13}C chemical shifts for [Pd([9]aneOS$_2$)Cl$_2$] in d_6-DMSO solution

	20°C (ppm)	120°C(ppm)	shift(Δδ)	%
-C*H$_2$O	76.65	75.35	1.30	1.70
-C*H$_2$S	42.71	42.26	0.45	1.05
-SC*H$_2$C*H$_2$S-	40.17	40.06	0.11	0.27

point to the same conclusion. As seen in Table 3-4, changes in ^{13}C chemical shift are very small (only 0.27 to 1.70%). These observations are consistent with the hypothesis that during the fluxional process the sulfur atoms maintain their equatorial location, and the oxygen atom remains in its roughly apical site.

Solvent apparently plays an important role in this fluxional process. The temperature-dependent ^1H NMR spectrum is only observed in dimethyl sulfoxide (DMSO), one of the dipolar aprotic solvents. To further examine the contribution of DMSO to the fluxional process, we added 10% (volume) of d_6-DMSO to the d_5-nitrobenzene solution of Pd([9]aneOS$_2$)Cl$_2$. As expected, the fine structure of ^1H NMR spectrum was quenched at 120°C by the addition (Fig. 3-5). This observation provides strong evidence for a solvent-assisted fluxional process.

The coordination capability of DMSO to transition metal ions is well studied [16,17]. As an ambidentate donor, DMSO

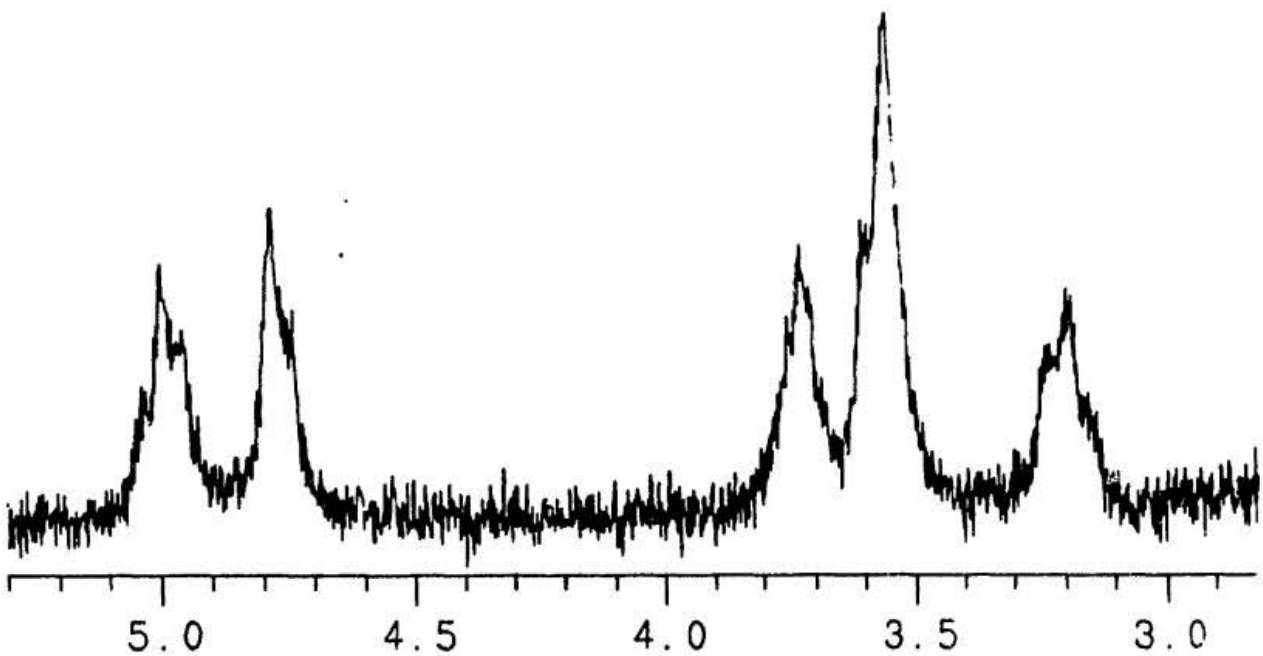

Fig. 3-5. ^{1}H NMR spectra of [Pd([9]aneOS$_2$)Cl$_2$] in d_5-nitrobenzene solution with 10% d_6-DMSO at 120°C

forms complexes with many metals by coordinating through oxygen, while for late transition metal ions such as Pd(II), Pt(II) or Ir(III), the sulfoxide ligand is usually bound to the metal through sulfur. For example, X-ray crystal structure determinations of $[PdCl_2(DMSO)_2]$ and $[Pd(NO)_2(DMSO)_2]$ reveal sulfur coordination in these Pd(II) complexes [18,19].

Finally, we examine the process (4) - a dissociation-recombination mechanism. After the preceding analysis, this pathway apparently makes itself more acceptable than other pathways. As sketched in Scheme 3-4, this mechanism would be expected to involve solvent nucleophilic attack and a ligand inversion process.

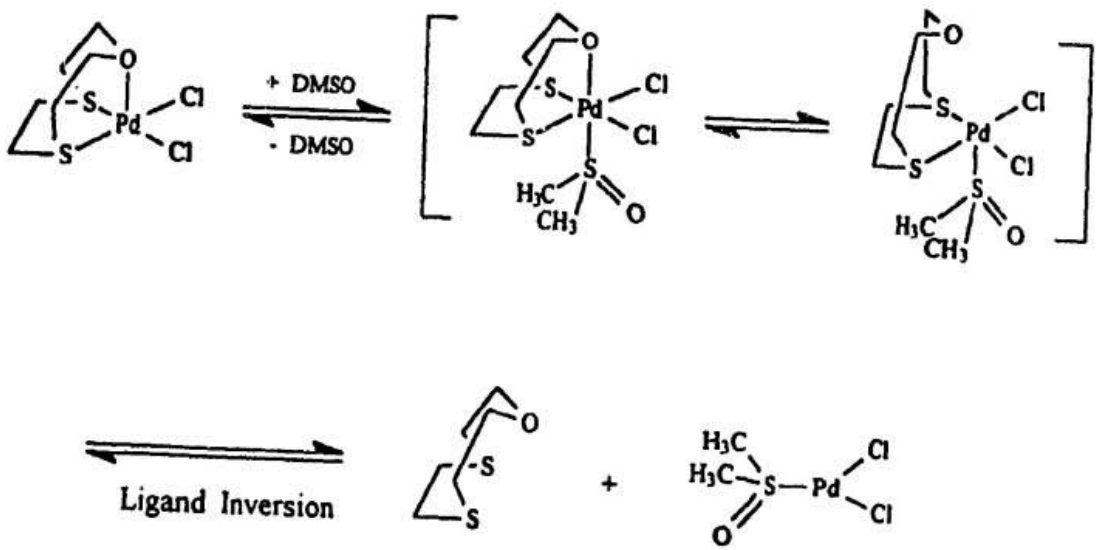

Scheme 3-4

When the temperature increases, the fluxional process begins with solvent attack. Since there is a open position opposite to the oxygen donor, Pd(II) ion exhibits its preference for Pd-S bonding in this site. DMSO attacks the Pd atom through the sulfur atom and forms an octahedral intermediate. The intermediate is unstable because it has 20 electrons and then quickly lose the O donor to form an 18 electron intermediate. As the temperature continues to rise, the complex decomposes and [9]aneOS$_2$ molecule becomes a free ligand, and then after the ligand inversion, [9]aneOS$_2$ recombines with the Pd atom to reform the complex. The inversion taking place in the free ligand state averages all the methylene proton signals in the ^{1}H NMR spectra, but the life time of free ligand is too short to be detected by ^{1}H NMR.

This mechanism is fully consistent with the ^{1}H and ^{13}C NMR spectral changes. From Table 3-3 it can be seen that the ^{13}C chemical shifts at 22°C and 120°C differ by 0.27, 1.1, and 1.7% for -(CH$_2$S)$_2$-, -CH$_2$S- and -CH$_2$O- respectively. These changes support the mechanism involving DMSO nucleophilic attack. After solvent attack the O donor is dissociated first, and following that a conformational inversion process may take place that moves the O atom from an endodentate to an exodentate position. A similar conformation change was introduced to explain the observation of fluxionality in [PtRR'([9]aneS$_3$)] [20]. This is consistent with the observation of the greatest change in the

^{13}C NMR spectrum occurring in the $-CH_2O-$ group. Meanwhile, the solvent peak (quintet, 39.50 ppm for d_6-DMSO) remains unchanged over the temperature range. This excludes the possibility of the chemical shift changes being due to thermal broadening effects in these ^{13}C spectra, and verifies that the spectral changes originate in the ligand.

The observed structural non-rigidity in [Pd([9]aneOS$_2$)Cl$_2$] may be due to the weak Pd-O bond in the distorted square-pyramidal structure, which could make [Pd([9]aneOS$_2$)Cl$_2$] susceptible to the fluxional activity.

3.4. Conclusion

Although ligand fluxions of cyclic chalcogen ligands have been reported previously [15,20,24], [Pd([9]aneOS$_2$)Cl$_2$] provides, to our knowledge, the first example of ligand fluxion involving a hard O-donor in a macrocyclic chalcogen ligands. Fluxionality with the participation of oxygen atoms is also unknown to date in complexes of acyclic chalcogen ligands. The intermolecular fluxional process involving ligand inversion is different from the reported 1,4-shift mechanism in Pd(II) complexes of crown thioether.

3.5. References

1. Blake, A.J.; Holder,A.J.; Robert, Y.V.; Schröder, M.; Acta Cryst. *44C*, 360(1988).
2. Wilkinson, G., Comprehensive Coordination Chemistry, vol.5, Pergamon Press, Elmsford, New York, P1144(1987).
3. Aires, B.E.; Ferguson, J.E.; Howarth, D.P.; Miller, J.M.; J. Chem. Soc., A, 1144(1971).
4. Ferguson, J.E.; Loh, K.S., Aust. J. Chem., *26*, 2615(1973).
5. Boeyens, J.C.A.; Dobson, S.M., Sterochemistry of Organometallic and Inorganic Compounds. Bernal, I. ed., vol.2, Elsevier, Amsterdam, P26(1987).
6. Hancock, R.D.; Dobson, S.M.; Boeyens, J.C.A., Inorg. Chim. Acta, *133*, 221(1987).
7. Abel, E.W.; Klan, A.R.; Kite, K.; Orrell, K.G. and Sik, V., J. Chem. Soc., Dalton Trans. 1175(1980).
8. Abel, E.W.; Bhargava, S.K.; Kite, K.; Orrell, K.G.; Sik, V. and Williams, B.L., Polyhedron, *1*, 289(1982).
9. Abel, E.W.; Khan, A.R.; Kite, K.; Orrell, K.G.; Sik,V., J. Chem. Soc., Dalton Trans., 2208(1980).
10. Abel, E.W.; Orrell, K.G., Prog. Inorg. Chem., *32*, 1(1989).
11. Orrell, K.G., Coord. Chem. Rev., *96*, 1(1989).
12. Berry, R.S., J. Chem. Phys., *32*, 933(1960)
13. Holmes, R.R., Prog. Inorg. Chem., *32*, 119(1984).
14. Wood, J.S., Prog. Inorg. Chem., *16*, 256(1972).

15. Abel, E.W.; Beer, P.D.; Moss, I.; Orrell, K.G.; Sik, V.; Bates, P.A. and Hursthouse, M.B., J. Chem. Soc., Chem. Commun., 978(1987).

16. Davies, J.A., Adv. Inorg. Chem. Radiochem., *24*, 115(1981).

17. (a) Cotton, F.A.; Francis, R., J. Am. Chem. Soc., *82*, 2986(1960). (b) Cotton, F.A.; Francis, R. and Horrocks, W.D., J. Phys. Chem., *64*, 1534(1960). (c) Selbin, J.; Bull, W.E. and Holmes, L.H., J. Inorg. Nucl. Chem., *16*, 219 (1961).

18. Bennett, M.J.; Cotton, F.A.; Weaver, D.L., Williams, R.J.; Watson, W.H., Acta Crystallogr., *23*, 788(1967).

19. Langs, D.A.; Hare, C.R. and Little, R.G., Chem. Commun., 1080(1967).

20. Bennett, M.A.; Canty, A.J.; Felixberger, J.K.; Rendina, L.M.; Sunderland, C.; Willis, A.C., Inorg. Chem., *32*, 1951 (1993).

21. Cheng, C.H.; Spivack, B.D.; Eisenberg, R., J. Am. Chem. Soc., *99*, 3003(1977).

22. Chisholm, M.H.; Tan, L.S.; Huffman, J.C., J. Am. Chem. Soc., *104*, 4879(1982).

23. Wood, J.S., "Sterochemical and Electronic Structural Aspects of Five-Coordination", Progress in Inorganic Chemistry, *16*, 227(1972).

24. Liu, S.; Lucas, C.R.; Newlands, M.J.; Charland, J.P., Inorg. Chem., *29*, 4380(1990).

Chemistry, *16*, 227(1972).

24. Liu, S.; Lucas, C.R.; Newlands, M.J.; Charland, J.P., Inorg. Chem., *29*, 4380(1990).
25. Abel, E.W.; Bush, R.P.; Hopton, F.J.; Jenkins, C.R., J. Chem. Soc., Chem. Commun., 58(1966).
26. Blake, A.J.; Holder, A.J., Hyde, T.I.; Kuppers, H.J.; Schröder, M.; Stozel, S.; Wieghardt, K.J., J. Chem. Soc., Chem. Commun., 1600(1990).
27. Wieghardt, K.; Küppers, H.J.; Raabe, E.; Krüger, C., Angew Chim. Int. Ed. Engl., *25*, 1101(1986).
28. Lucas, C.R.; Liu, S.; Newlands, M.J.; Gabe, E.J., Can. J. Chem., *68*, 1357(1990).
29. Okeya, S.; Miyamoto, T.; Ooi, S.; Nakamura, Y.; Kawaguchi, S., Inorg. Chim. Acta, *45*, L135(1980).
30. Siedle, A.R.; Newmark, R.A.; Pignolet, L.H., J. Am. Chem. Soc., *103*, 4947(1981).
31. Louis, R.; Pelissard, D.; Weiss, R., Acta Cryst., *B30* , 1889(1974).
32. Siedle, A.R.; Newmark, R.A.; Pignolet, L.H., J. Am. Chem. Soc., *103*, 4947(1981).
33. Okeya, S.; Asai, H.; Ooi, S.; Matsumoto, K.; Kawaguchi, S.; Kuroya, H., Inorg. Nucl. Chem. Lett., *12*, 677(1976).
34. Okeya, S.; Ooi, S.; Matsumoto, K.; Nakamura, Y.; Kawaguchi, S., Bull. Chem. Soc. Jpn., *54*, 1085(1981).
35. Holmes, P.R., Pentacoordinated Phosphorus, Vol.1, ACS

IV. Synthesis and Properties of $[Cu([9]aneOS_2)_2]ClO_4$

4.1. Experimental Section

Tetrakis(acetonitrile)copper(I) perchlorate was prepared by the published method [1]. Other reagents were obtained from the Aldrich Chemical Co. Inc. or Alfa Products Inc. and were used without further purification. Spectroscopic data were obtained using the following instruments: IR, Mattson Polaris; NMR, General Electric 300-NB. X-ray data were collected by using a Rigaku AFC6S diffractometer. Electrochemical measurements were carried out under a nitrogen atmosphere at room temperature by using a Cypress Systems, Inc., CS-1087 computer controlled potentiostat. Solution concentrations were 10^{-3} mol/L in complex and 10^{-1} mol/L in supporting electrolyte (tetraethylammonium perchlorate). Voltammograms were recorded in acetonitrile by using a platinum working electrode, a platinum counterelectrode, and an aqueous saturated calomel reference electrode (SCE).

4.1.1. Preparation of $[Cu([9]aneOS_2)_2][ClO_4]CH_3CN$

A solution of $[Cu(CH_3CN)_4]ClO_4$ (65 mg, 0.20 mmol) in 10 ml of acetonitrile was added to a solution of $[9]aneOS_2$ (65 mg, 0.40 mmol) in 5 ml of acetonitrile under a nitrogen atmosphere. The mixture was stirred at 50°C for 2 h. The resulting yellow-green solution was filtered and left to evaporate slowly. Colourless crystals were collected by filtration, washed well with dichloromethane, and dried under vacuum overnight. Yield 83.5 mg (78.4%). IR (cm^{-1}, KBr, Nujol): 2922(vs), 2655(vs), 2245(m), 1465(s), 1411(m), 1377(m), 1296(m), 1264(m), 1229(w), 1182(w), 1133(s), 1062(vs), 1009(s), 926(m), 847(vw), 818(w), 722(vw), 658(vw), 622(s), 470(vw), 441(w). ^1H NMR (ppm from TMS internal standard, CD_3CN): 3.85(t, 4H, CH_2O), 3.07(s, 4H, SCH_2CH_2S), 2.81(t, 4H, CH_2S), 1.93(m, CH_3CN). Anal. calcd. for $C_{14}H_{27}ClCuNO_6S_4$: C 31.57, H 5.12, N 2.62; found: C 31.69, H 5.12, N 2.57.

4.1.2. X-ray Crystallography

Crystals suitable for X-ray analysis were obtained by slow vapour diffusion of diethyl ether into a solution of the perchlorate salt of the complex in acetonitrile. All measurements were made on a Rigaku AFC6S diffractometer with

Table 4-1. Crystal Data for $[Cu([9]aneOS_2)_2][ClO_4]CH_3CN$

chem formula	$C_{14}H_{27}ClCuNO_6S_4$	V(Å^3)	2212.4(9)
fw	532.26	Z	4
space group	P2/n (No.14)	ρ_{calcd}(g cm^{-1})	1.599
a(Å)	7.743(2)	μ(cm^{-1})	15.02
b(Å)	19.515(5)	λ(Å)	0.71069
c(Å)	15.017(2)	R	0.036
β(deg)	102.85(2)	R_w	0.038
T(°C)	26		

graphite monchromated Mo Kα radiation. The crystallographic data are presented in Table 4-1.

4.2. Results and Discussion

4.2.1. Crystal Structure of $[Cu([9]aneOS_2)_2][ClO_4]CH_3CN$

The ORTEP diagram of the complex cation $[Cu([9]aneOS_2)_2]^+$ with atomic labelling for the non-hydrogen atoms is shown in Fig. 4-1. Selected bond lengths and angles are presented in Table 4-2.

The copper(I) ion is coordinated by two pairs of sulfur atoms from two [9]aneOS$_2$ molecules so that the coordination geometry of the copper(I) ion is tetrahedral. The Cu-S a

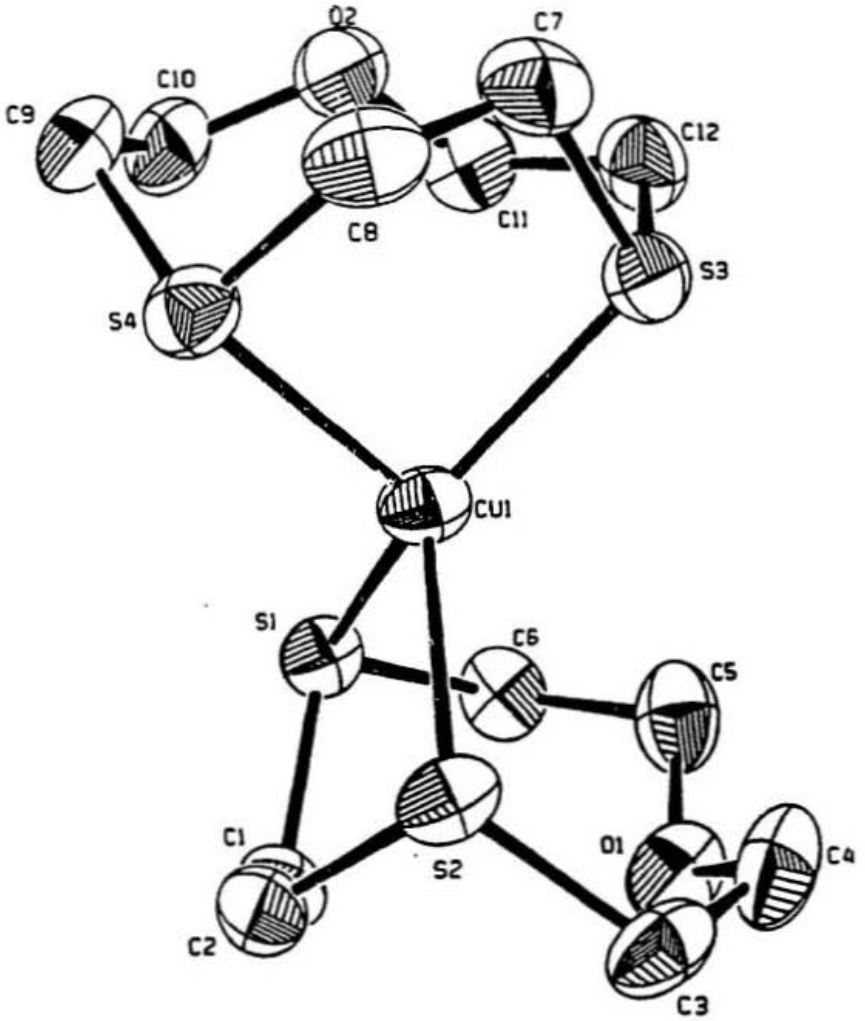

Fig. 4-1. The structure of $[Cu([9]aneOS_2)_2]^+$ in $[Cu([9]aneOS_2)_2][ClO_4]CH_3CN$

Table 4-2. Selected Geometrical Parameters for $[Cu([9]aneOS_2)_2]^{2+}$

Intramolecular Distances (Å)

atom	atom	distance	atom	atom	distance
Cu(1)	S(1)	2.302(1)	S(4)	C(8)	1.815(5)
Cu(1)	S(2)	2.356(1)	S(4)	C(9)	1.830(4)
Cu(1)	S(3)	2.292(1)	O(1)	C(4)	1.418(5)
Cu(1)	S(4)	2.345(1)	O(1)	C(5)	1.411(5)

Intramolecular Bond Angles (deg.)

atom	atom	atom	angle	atom	atom	atom	angle
S(1)	Cu(1)	S(2)	92.99(4)	S(1)	Cu(1)	S(3)	130.20(5)
S(1)	Cu(1)	S(4)	115.10(4)	S(2)	Cu(1)	S(3)	119.86(5)
S(2)	Cu(1)	S(4)	103.88(4)	S(3)	Cu(1)	S(4)	93.53(4)

Torsion Angles for $[9]aneOS_2$ Ring (deg.)

atoms				angle	atoms				angle
S(3)	C(7)	C(8)	S(4)	-46.3(4)	S(3)	C(12)	C(11)	O(2)	58.0(4)
S(4)	C(9)	C(10)	O(2)	-66.9(4)	C(1)	S(1)	C(6)	C(5)	-76.9(3)
S(1)	C(1)	C(2)	S(2)	-49.5(4)	C(1)	C(2)	S(2)	C(3)	-68.2(3)
S(1)	C(6)	C(5)	O(1)	60.8(4)	C(2)	S(2)	C(3)	C(4)	97.1(3)
C(2)	C(1)	S(1)	C(6)	129.8(3)	C(3)	C(4)	O(1)	C(5)	134.2(4)
C(4)	O(1)	C(5)	C(6)	-141.4(4)	C(7)	S(3)	C(12)	C(11)	-77.0(4)

(continued)

C(7)	C(8)	S(4)	C(9)	-70.0(4)	C(8)	S(4)	C(9)	C(10)	94.7(4)
S(2)	C(3)	C(4)	O(1)	-68.5(4)	C(8)	C(7)	S(3)	C(12)	128.7(3)
C(9)	C(10)	O(2)	C(11)	137.5(4)	C(10)	O(2)	C(11)	C(12)	-141.5(4)

distances range from 2.292(1) to 2.345(1) Å with an average length of 2.324 Å. These results compare well with those from [Cu(3,6-dithiaoctane)$_2$]$^+$ [2] which varied from 2.280(4) Å to 2.318(5) Å with an average of 2.303 Å and those from [CuL$_2$]$^+$ (L=2,5,8-trithia[9](2,5)thiophenophane) [3] which range from 2.301(3) Å to 2.392(3) Å with an average of 2.340 Å.

The angles about the copper atom vary from 92.99(4) to 130.20(5)°. The distortions from the ideal tetrahedral angles arise mainly from constraints within the macrocyclic rings. As two coordinated sulfur atoms come from the same ligand, the S-Cu-S angle is compressed to about 93° which is often found in five-membered chelate rings of copper(I) [2-4]. When the sulfur atoms are in different ligand molecules, the S-Cu-S angles are close to the tetrahedral values (except one with ~ 130°) (Table 4-2). These two types of angles are often observed in [2+2] coordination of copper(I) complexes [2,3].

The [2+2] coordination of [Cu([9]aneOS$_2$)$_2$]$^+$ is different from [Cu([9]aneS$_3$)$_2$]$^+$ which has [3+1] coordination geometry [5].

The difference can be explained by the preference of copper(I) for soft S-donors over hard O-donors, so [9]aneOS$_2$ is not able to adopt a facial coordination conformation as [9]aneS$_3$ does. The macrocyclic ligand has a [234] conformation (Table 5-2), whereas the [333] conformation was observed in [Cu([9]aneS$_3$)$_2$]$^+$. The three hetero-atoms adopt an up-up-down arrangement and the uncoordinated oxygen atom is orientated away from the metal centre. This conformation is similar to conformation **II** of the free ligand obtained from molecular mechanics calculations (Chapter II), but differs from [Pd([9]aneOS$_2$)Cl$_2$] in which the ligand adopts facial coordination conformation (Chapter III). These observations indicate the [9]aneOS$_2$ molecule is a considerably flexible ligand. The torsion angles for C-C-O-C in the two copper-bound ligand molecules range from 134.2(4) to 141.5(4)°, is consistent with the preference of oxygen atoms for anti-placement (see Chapters I and II).

4.2.2. IR Spectrum

The IR spectrum shows strong bands at 1062 cm^{-1} and 622 cm^{-1} corresponding to the characteristic vibrational frequencies of the perchlorate ion [5]. A band at 2245 cm^{-1} is typical of ν(C≡N) in the uncoordinated CH$_3$CN molecule [6].

4.2.3. Electrochemistry

Cyclic voltammetry of $[Cu([9]aneOS_2)_2]ClO_4$ (Fig. 4-2) reveals a quasi-reversible one electron wave at +0.607 V vs. SCE, with ΔE_p of 0.114 V at a scan rate of 110 mV/s (the ferrocenium/ferrocene potential under the similar conditions was 0.437 V with ΔE_p=0.081 V). No other waves appear within the potential limit of the solvent and solutions of the free ligand show no redox activity in the voltage range 0.0-1.0 V vs. SCE under the same conditions.

The observation of a quasi-reversible process instead of a reversible one indicates the likehood that the Cu^{II}/Cu^{I} redox process is accompanied by a change of coordination number, and this is strongly supported by the independent synthesis of $[Cu([9]aneOS_2)_2](ClO_4)_2$. By comparison to $[Cu(14S4)(OClO_3)]^{2+}$ which is known to adopt pseudo-octahedral geometry [7], $[Cu([9]aneOS_2)_2]^{2+}$ probably also is pseudo-octahedral because electronic spectra are very similar (for $[Cu(14S4)(OClO_3)_2]$: 390 nm (8200 $M^{-1}cm^{-1}$) and 570 nm (1900 $M^{-1}cm^{-1}$); for $[Cu([9]aneOS_2)](ClO_4)_2$: 390 nm (2700 $M^{-1}cm^{-1}$) and 560 nm (280 $M^{-1}cm^{-1}$)). Because bond formation/cleavage is typically slower than electron transfer, whereas reversible behaviour requires that electron transfer determine the rate of the redox process [8], it is expected that any change of coordination geometry a

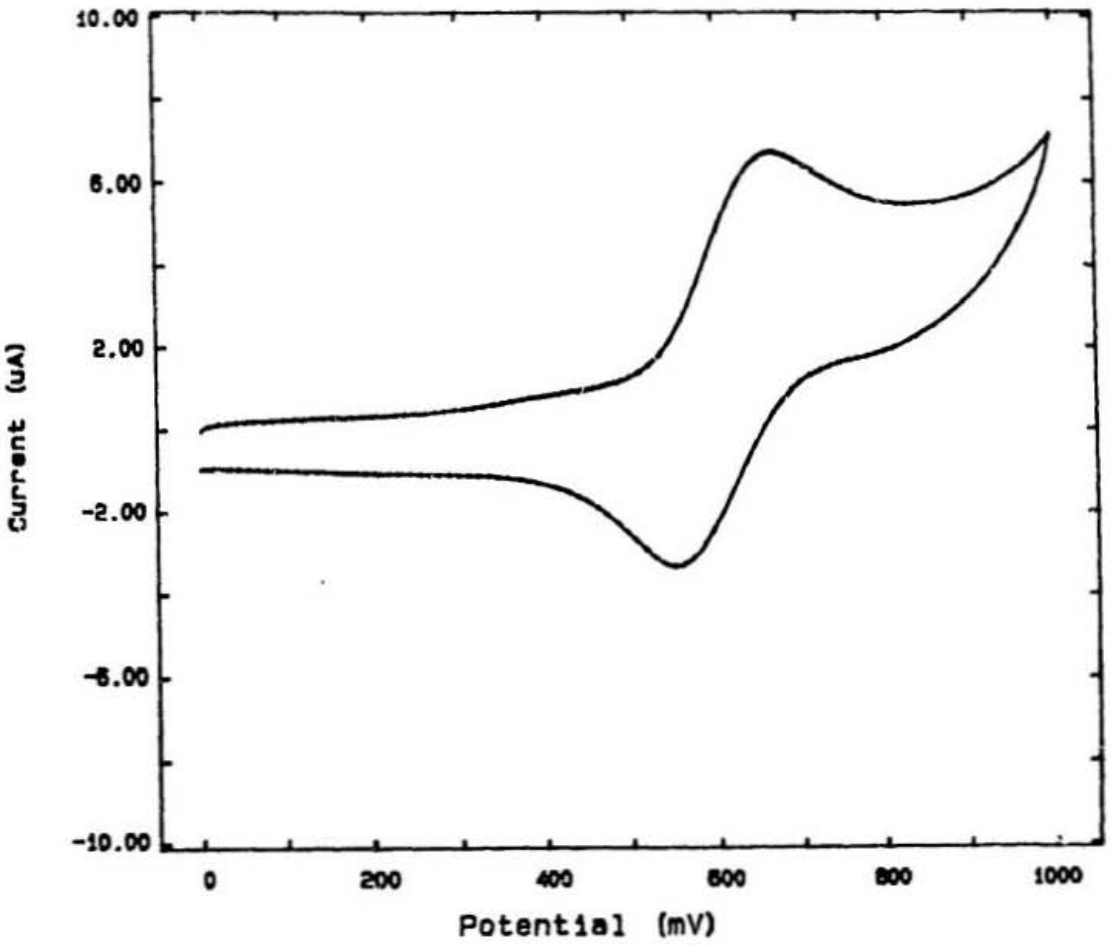

Fig. 4-2. The cyclic voltammogram of $[Cu([9]aneOS_2)_2]ClO_4CH_3CN$ in CH_3CN (platinum working electrode, platinum wire counter electrode and SCE reference electrode) at scan rate of 110 mV/s.

will disturb the reversible process.

Though measured under somewhat different conditions, a series of Cu(II) complexes of thioethers (both linear and macrocyclic ligands) shows redox potentials for the Cu^{II}/Cu^{I} couple ranging from +0.46 to +0.72 V vs. SCE [9-11]. The relatively high redox ptential of $[Cu([9]aneOS_2)_2]^+$ (+0.607 V vs. SCE) suggests the ligand [9]aneOS$_2$ considerably stabilizes Cu(I) over Cu(II).

It is notable that octahedral $[Cu([9]aneS_3)_2]^{2+}$ was reduced in a quasi-reversible fashion at +0.61 V vs. SCE [10] which is almost the same redox value as that of $[Cu([9]aneOS_2)_2]^+$. Recent electrochemical studies reveal that redox processes of the $[Cu([9]aneS_3]^{2+}/[Cu([9]aneS_3)]^+$ system follow an ECEC mechanism rather than a simple electron transfer mechanism. A square ECEC mechanism was proposed to account for the changes in coordination geometry associated with electron transfer [14].

For the $[Cu([9]aneOS_2)]^{2+}/[Cu([9]aneOS_2)]^+$ couple, it should be borne in mind that there is one hard O-donor in the [9]aneOS$_2$ ligand. Since $[Cu([9]aneOS_2)_2]^{2+}$ probably adopts octahedral geometry like $[Cu(14S4)(OClO_3)]^{2+}$ [7], it is possible that the oxygen donor in [9]aneOS$_2$ will participate in the redox process, though there is not clear experimental evidence so far to support this. In contrast to the much higher potentials found for complexes with thioethers, typical Cu^{II}/Cu^{I} couples with

nitrogen- or oxygen-donor ligands exhibit redox potentials between -0.7 and 0 V vs. SCE [12]. It is interesting to find that the copper complexes of [9]aneS_3 and [9]aneOS_2 have almost the same redox potentials. This observation suggests that an oxygen donor might have a similar effect as a sulfur donor in manipulating the redox potential of the Cu^{II}/Cu^{I} couple in a coordination environment mainly comprising thioethers. This discovery is helpful in comprehending the function of some metal-containing redox proteins function such as, for example, the "blue" copper-containing oxidases [13].

4.3. References:

1. Kubas, G.J., Inorg. Synth., *19*, 90 (1979).
2. Baker, E.N.; Norris, G.E., J. Chem. Soc., Dalton Trans., 877 (1977).
3. Lucas, C.R.; Liu, S.; Newlands, M.J, Can. J. Chem., *66*, 1506 (1988).
4. Corfield, R.W.R.; Ceccarelli, C.; Glick, M.D.; Moy, I.W.Y.; Ochrymowycz, L.A.; Rorabacher, D.B., J. Am. Chem. Soc., *107*, 2399 (1985).
5. Nyquist, R.A.; Kagel, R.D., Infared Spectra of Inorganic Compounds, Acdemic Press, New York, NY, P17 (1971).

6. Nakamoto, K., Infrared and Raman Spectra of Inorganic and Coordination Compounds, John Wiley & Sons, Inc., New York, NY, P280 (1986).

7. Rorabacher, D.B.; Bernado, M.M.; Vande Linde, A.M.Q.; Leggett, G.H.; Westerby, B.C.; Martin, D.J.; Ochrymowycz, L.A., Pure Appl. Chem., *60*, 501 (1988).

8. Headridge, J.B., Electrochemical Techniques for Inorganic Chemist, Acdemic Press, London, 1969.

9. Karlin, K.D.; Zubieta, J., Eds., Copper Coordination Chemistry: Biological and Inorganic Perspectives, Adenine Press, Guiderland, NY, P167-202 (1983).

10. Hartman, J.R.; Cooper, S.R., J. Am. Chem. Soc., *108*, 1202 (1986).

11. Dockal, E.R.; Jones, T.E.; Sokol, W.F.; Energer, R.J.; Rorabacher, D.B., J. Am. Chem. Soc., *98*, 4322 (1976).

12. Patterson, G.S.; Holm, R.H., Bioinorg. Chem., 4, 257 (1975).

13. Kano, S.K.; Glass, R.S.; Wilson, G.S., J. Am. Chem. Soc., *115*, 592 (1993).

14. Kano, S.K.; Glass, R.S. and Wilson, G.S., J. Am. Chem. Soc., *115*, 592 (1993).

V. Synthesis and Properties of $[Cu([9]aneOS_2)Br]_2$

5.1. Preparation of $[Cu([9]aneOS_2)Br]_2$

A solution of CuBr (72 mg 0.50 mmol; Aldrich Chemical Co. Inc.) in 15 ml of acetonitrile was added to a solution of [9]aneOS$_2$ (98 mg, 0.57 mmol) in 20 ml of acetonitrile. The solution colour changed from green to light brown and a yellow precipitate was formed. The precipitate disappeared after the mixture was refluxed for 2 h. with stirring. The solution was allowed to cool to room temperature resulting in precipitation of a grey crystalline solid. The precipitate was separated, washed with ethanol, and recrystallized from acetonitrile to give 108 mg (70%) of $[Cu([9]aneOS_2)Br]_2$ as colourless crystals. IR (cm, KBr, Nujol): 2923(vs), 2855(vs), 1461(s), 1410(m), 1378(s), 1357(m), 1304(m), 1261(m), 1224(m), 1133(s), 1004(m), 923(m), 843(m), 813(w), 781(w), 722(w), 665(w), 613(w), 474(w), 440(m). Anal. calcd. for $C_6H_{12}OCuBrS_2$: C 23.42, H 3.93; found: C 23.58, H 3.93.

5.2. Results and Discussion

5.2.1. Descriptions of the Structure

The ORTEP perspective drawing of $[Cu([9]aneOS_2)Br]_2$ with

Table 5-1. Crystal Data for $[Cu([9]aneOS_2)Br]_2$

chem formula	$C_6H_{12}OCuBrS_2$	V(Å^3)	508.1(4)
fw	307.73	Z	2
space group	P1(No.2)	ρ_{calcd}(g cm^{-1})	2.011
a(Å)	7.808(5)	μ(cm^{-1})	63.93
b(Å)	8.880(3)	λ(Å)	0.71096
c(Å)	7.567(2)	R	0.027
α(deg)	92.44(3)	R_w	0.027
β(deg)	100.32(3)	T(°C)	26
γ(deg)	99.30(4)		

Table 5-2. Selected Geometrical Parameters for $[CuBr([9]aneOS_2)]_2$

Intramolecular Distances (Å)					
atom	atom	distance	atom	atom	distance
Br(1)	Cu(1)	2.557(1)	Br(1)	Cu(1)	2.392(1)
O(1)	C(4)	1.414(5)	Cu(1)	S(1)	2.338(2)
O(1)	C(5)	1.410(5)	Cu(1)	S(2)	2.345(1)
C(1)	C(2)	1.437(7)	S(1)	C(1)	1.811(5)
C(3)	C(4)	1.500(7)	S(1)	C(6)	1.813(5)

Table 5-2 (continued)

C(5)	C(6)	1.507(7)	S(2)	C(2)	1.799(5)

Intramolecular Bond Angles (deg.)

atom	atom	atom	angle	atom	atom	atom	angle
Cu(1)	Br(1)	Cu(1)	70.28(4)	Cu(1)	S(2)	C(2)	95.9(2)
Br(1)	Cu(1)	Br(1)	109.72(4)	Cu(1)	S(2)	C(3)	113.5(2)
Br(1)	Cu(1)	S(1)	104.22(5)	C(2)	S(2)	C(3)	104.3(3)
Br(1)	Cu(1)	S(2)	99.34(5)	C(4)	O(1)	C(5)	116.4(4)
Br(1)	Cu(1)	S(1)	120.55(5)	S(1)	C(1)	C(2)	119.8(4)
Br(1)	Cu(1)	S(2)	126.47(4)	S(2)	C(2)	C(1)	121.5(4)
S(1)	Cu(1)	S(2)	92.76(6)	S(2)	C(3)	C(4)	114.6(3)

Torsion Angles (deg.)

atoms	angle	atoms	angle
Br(1)Cu(1)Br(1)Cu(1)	0	S(1) C(1) C(2) S(2)	32.3(7)
S(1) C(6) C(5) O(1)	-60.4(4)	Br(1)Cu(1)Br(1)Cu(1)	0
Cu(1)Br(1)Cu(1)Br(1)	0	S(2) C(3) C(4) O(1)	67.5(5)
Cu(1)Br(1)Cu(1)Br(1)	0	C(1) C(2) S(2) C(3)	79.8(5)
C(2) S(2) C(3) C(4)	-92.5(4)	C(2) C(1) S(1) C(6)	-120.0(5)
C(3) C(4) O(1) C(5)	-139.1(4)	C(4) O(1) C(5) C(6)	140.1(4)

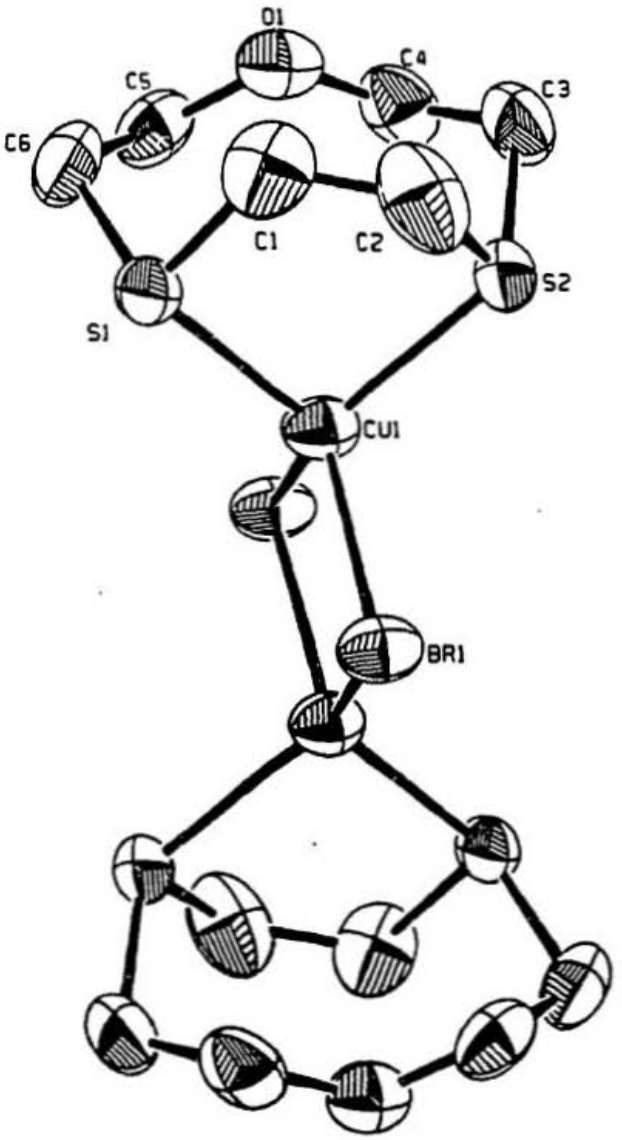

Fig. 5-1 The structure of $[Cu([9]aneOS_2)Br]_2$

atomic labelling for the non-hydrogen atoms is shown in Fig.5-1. The crystal data are presented in Table 5-1. Selected bond distances, angles , and torsion angles are in Table 5-2.

As illustrated in Fig. 5-1, the molecule of $[Cu([9]aneOS_2)Br]_2$ exists as a dimer and is centrosymmetric. The copper(I) centres are in a tetrahedral coordination environment and connected via two inequivalent bromide bridges (Cu-Br = 2.557(1) Å, and Cu-Br' = 2.392(1) Å). They are, in addition, each bonded to two sulfur donors from the macrocyclic ligand with bond lengths: Cu-S = 2.338(2) Å and Cu-S = 2.345(1) Å.

The bond angles around copper(I) deviate from those of standard tetrahedral geometry and range from 92.76(6)° to 126.47(4)°. Of these, the smallest is the compressed S-Cu-S angle, as we have seen previously in the case of $[Cu([9]aneOS_2)_2]^+$. The Cu(1)-S(2)-C(2) angle is also reduced to 95.9(2)° owing to constraints in the chelating ring.

Examination of the $Cu_2(\mu\text{-}Br)_2$ plane reveals a close Cu-Cu distance of 2.852(1) Å and a small Cu-Br-Cu' angle (70.28(4))°. The Cu-Cu distance is shorter than those found in $(NEt_4)_2[Cu_2Br_4]$ [1] and $[Cu_2(triphenylphosphine)_3Br_2]$ [2] (Cu-Cu = 2.937(3) Å and 2.992(2) Å , respectively), but longer than those of some copper(I)-iodide species like $[(AsPh_3)(MeCN)CuI]_2$ (Cu-Cu = 2.779(1) Å) [3]. Mehrotra and Hoffmann suggested that a Cu-Cu distance of 2.83 Å represents overlap populations of 0.32 (bonding energy -0.417 eV) from molecular orbital calculations

on tetrameric Cu_4^{4+} clusters [4]. Thus, the short Cu^I-Cu^I bond distance may represent a weak copper-copper interaction in the $[Cu([9]aneOS_2)Br]_2$ dimer.

5.2.2. Electrochemistry

The investigation of redox properties of $[Cu([9]aneOS)Br]_2$ was undertaken in acetonitrile by using a three-electrode cell system consisting of a platinum working electrode, an aqueous saturated calomel reference electrode (SCE), and a platinum counter-electrode. Solution concentrations were 10^{-3} mol/L in the complex and 10^{-1} mol/L in tetraethylammonium perchlorate as a supporting electrolyte. The cyclic voltammogram of dimeric $[Cu([9]aneOS_2)Br]_2$ is shown in Fig. 5-2.

Though the molecule contains two redox-active sites, only a single wave ($E_{1/2}$=0.594 V vs. SCE, scan rate: 110 mV/s) appears in the cyclic voltammogram. This indicates two oxidation reactions in $[Cu([9]aneOS_2)Br]_2$ may occur at the same potential ($E^0_1 = E^0_2$) according to the result [5]:

$$Cu^I\text{-}Cu^I \overset{E_1^\circ}{\rightleftharpoons} Cu^I\text{-}Cu^{II} \overset{E_2^\circ}{\rightleftharpoons} Cu^{II}\text{-}Cu^{II}$$

The electrochemical behaviour of molecules with two or more chemically equivalent and reversible redox centres has been the subject of theoretical and experimental studies [6-9].

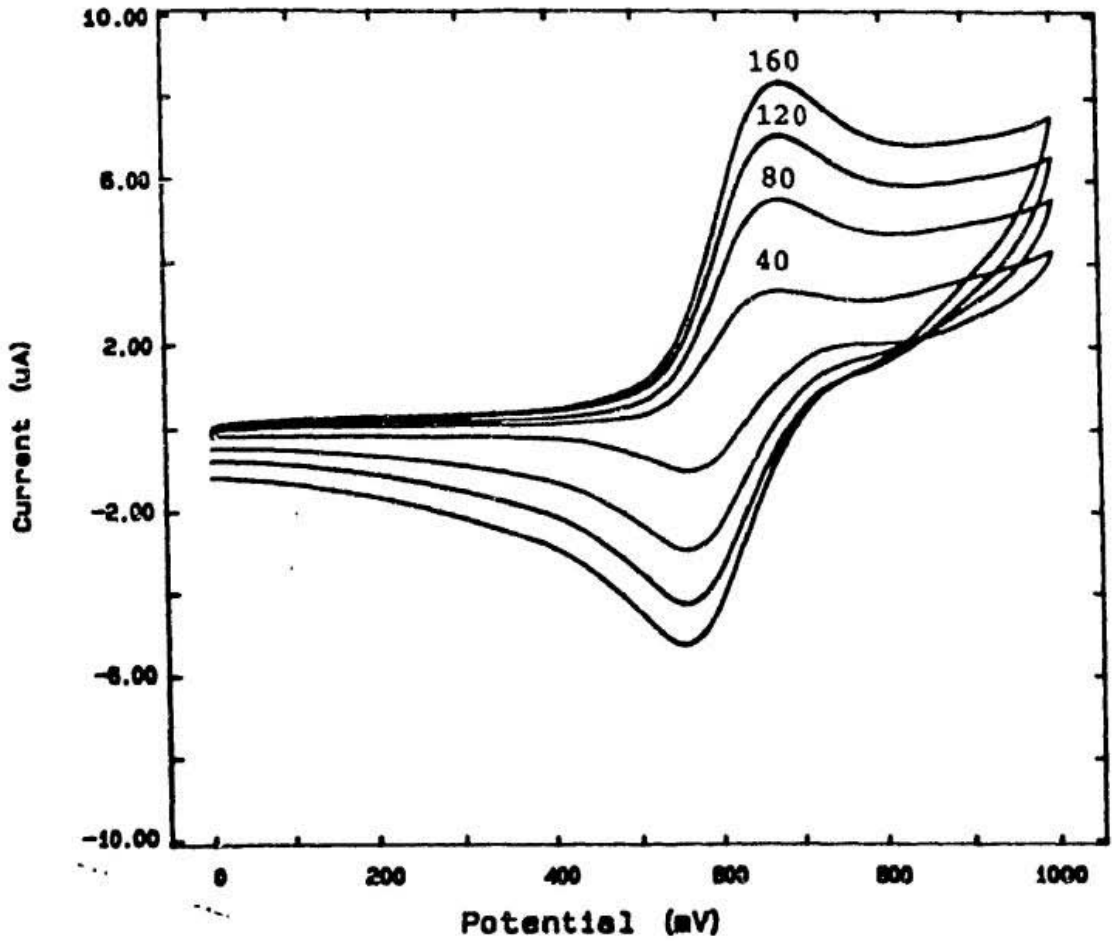

Fig. 5-2 Cyclic voltammograms of $[Cu([9]aneOS_2)Br]_2$ in CH_3CN (platinum working electrode, platinum wire counter electrode and SCE reference electrode) at scan rates: 40,80,120 and 160 mV/s.

If sequential electron transfer for both oxidations occurs at the same potential ($E^0_1 = E^0_2$), the theoretical peak separation for the reversible process should be 42 mV [10,11]. Though the separation of cathodic and anodic peaks for $[Cu([9]aneOS_2)Br]_2$ is about 100 mV, it does not change significantly with increasing scan rate (Fig. 5-2). Thus, the redox reactions in $[Cu([9]aneOS_2)Br]_2$ can be described as quasi-reversible. The deviation of these from a reversible redox process suggests that these redox reactions are not solely charge-transfer dominated. In fact, electron-transfer reactions coupled with chemical reactions are very frequent [12-15]. Thus, the present redox behaviour is better interpreted as following an ECE mechanism (C indicating chemical reactions which either precede or follow the charge transfers E) rather than a simple EE mechanism.

For the dinuclear bridged $[Cu([9]aneOS_2)Br]_2$, the two stepwise electron transfers (eq. 1) may cooperate with a disproportionation reaction (eq. 2) [16]:

$$Cu^I\text{-}Cu^I \rightleftharpoons Cu^I\text{-}Cu^{II} \rightleftharpoons Cu^{II}\text{-}Cu^{II} \qquad \text{eq.1}$$

$$2Cu^I\text{-}Cu^{II} \rightleftharpoons Cu^I\text{-}Cu^I + Cu^{II}\text{-}Cu^{II} \qquad \text{eq.2}$$

On the other hand, the bond forming and breaking during the charge-transfer process also needs to be taken into account. It is possible that oxidation of the tetrahedral Cu(I)

to Cu(II) will be associated with some change of coordination sphere. These structural changes will intervene unavoidably in the charge-transfer process, and therefore contribute to deviation from a reversible process.

5.3. References

1. Asplund, M.; Jagner, S., Acta Chem. Scand., Ser. A, *38*, 135 (1984).
2. Negita, H.; Hiara, M.; Kushi, Y.; Kuramoto, M.; Okuda, T., Bull. Chem. Soc. Jan., *54*. 1247 (1981).
3. Churchill, M.R.; Missert, J.R., Inorg. Chem., 20, 619 (1981).
4. Mehrotra, P.; Hoffmann, R., Inorg. Chem., 17, 2187 (1978).
5. Heinze, J., Angew. Chem. Int. Ed. Engl., *23*, 831 (1984).
6. Flanagan, J.B.; Mangel, S.; Bard, A.J.; Anson, F.C., J. Am. Chem. Soc., *100*, 4248 (1978).
7. Polcyn, D.S.; Shain, I., Anal. Chem., *45*, 2043 (1973).
8. Ammar, F.; Saveant, J.M., J. Electroanal. Chem., 47, 215 (1973).
9. Phaphs, J.; Bard, A.J., J. Electroanal. Chem., *68*, 313 (1976).
10. Rossiter, B.W. and Hamiton, J.F., Eds., Electrochemical Methods, John Wiley & Sons Inc., New York, NY,

P326 (1986).

11. Fenton, D.E.; Lintvedt, R.L., J. Am. Chem. Soc., *100*, 6367 (1978).
12. Gosser, D.K., Cyclic Voltammetry: Simulation and Analysis of Reaction Mechanisms, VCH Publisher, Inc., New York, NY, P74 (1994).
13. Novel, M.; Vasu, K.I.; Cyclic Voltammetry and the Frontiers of Electrochemistry, Aspect Publications Ltd., London, P196-260 (1990).
14. Andrieux, C.P.; Nadjo, L.; Saveant, J.M., J. Electoanal. Chem., *26*, 147 (1970).
15. Nicholson, R.S.; Shain, I., Anal. Chem., *37*, 178 (1965).
16. Ryan, M.D., J. Electrochem. Soc., *125*, 547 (1978).

VI. Synthesis and characterisation of $[Ag([18]aneO_2S_4)]ClO_4$

6.1. Preparation of $[Ag([18]aneO_2S_4)]ClO_4$

A solution of $AgClO_4xH_2O$ (20.7 mg, ~ 0.1 mmol, Aldrich Chemical Co. Inc.) in 5 ml of methanol was added to a solution of $[18]aneO_2S_4$ (32.8 mg. 0.100 mmol) in 5 ml dichloromethane immediately resulting in a white precipitate. The white solid dissolved after stirring for 30 min. at 50°C. The clear solution was left standing in air to allow slow evaporation of solvent. The resulting white solid was washed well with dichloromethane, and dried in vacuum overnight. Yield 44.1 mg (82.3%). IR (cm^{-1}, KBr, Nujol): 2923(vs), 2854(vs), 1465(vs), 1377(s), 1260(s), 1141(s), 1116(s), 1027(s), 962(m), 915(m), 836(m), 776(w), 755(m), 722(w), 636(m), 571(m), 514(m), 493(w), 434(w). Anal. cacd. for $C_{12}H_{24}AgClO_6S_4$: C 26.90, H 4.51; found: C 27.08, H 4.56.

6.2. Results and Discussion

6.2.1. Structure of $[Ag([18]aneO_2S_4)]ClO_4$

A crystal suitable for x-ray diffraction measurements was obtained by vapour diffusion of diethyl ether into a solution of $[Ag([18]aneO_2S_4)]ClO_4$ in nitromethane. All measurements were made on a Rigaku AFC6S diffractometer with graphite monochromated Mo

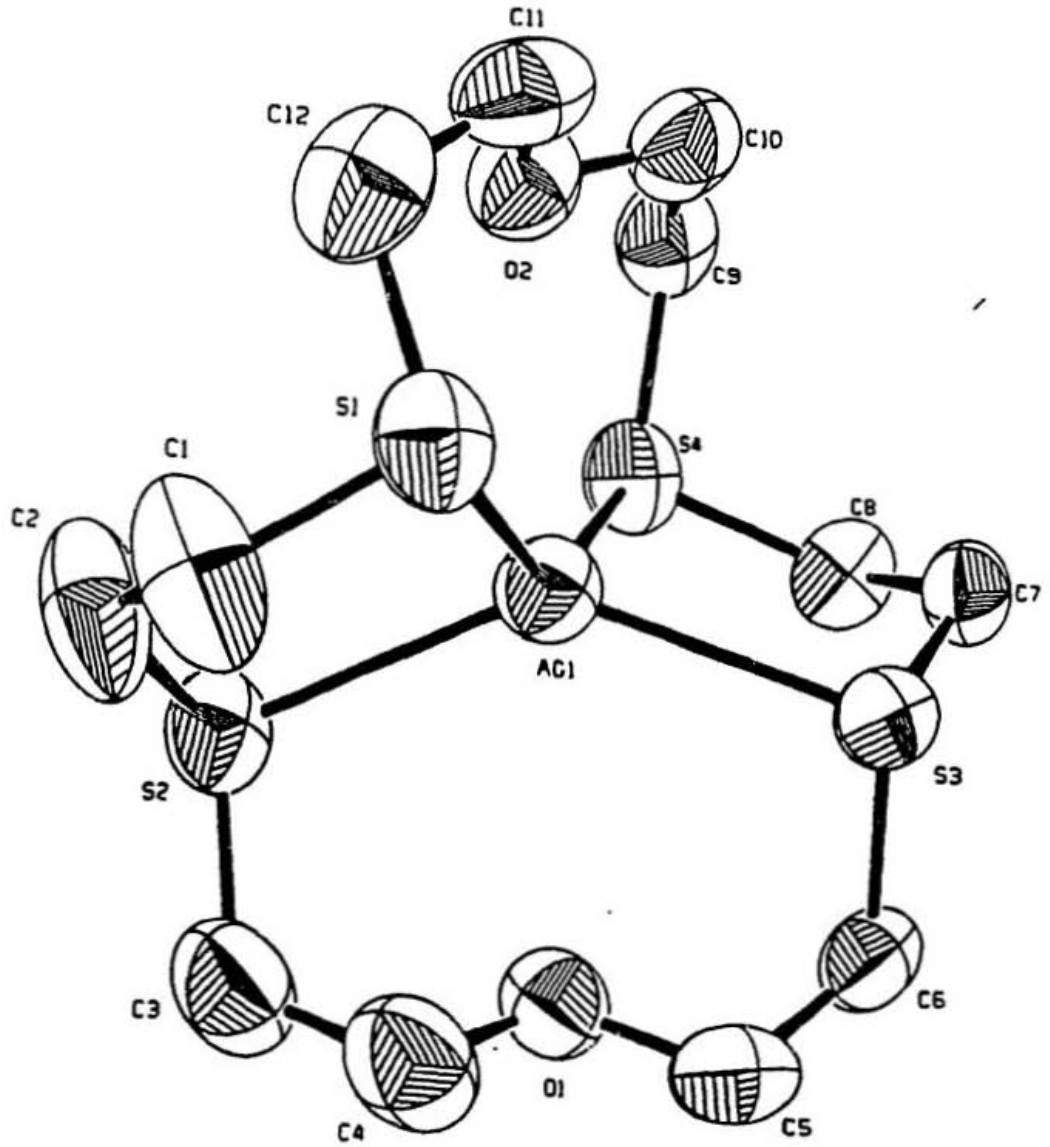

Fig. 6-1. The structure of the $[Ag([18]aneO_2S_4)]^+$

Kα radiation and a 2 KW sealed tube generator. The crystallographic data are presented in Table 6-1.

An ORTEP drawing of the complex cation $[Ag([18]aneO_2S_4)]^+$ is shown in Fig. 6-1. Bond lengths and angles are presented in

Table 6-1. Crystal Data for $[Ag([18]aneO_2S_4)]ClO_4$

chem formula	$C_{12}H_{24}AgClO_6S_4$	V(Å^3)	2023.3(7)
fw	535.88	Z	4
space group	$P2_1/C$(No.14)	ρ_{calcd}(g cm^{-1})	1.759
a(Å)	9.089(2)	μ(cm^{-1})	15.39
b(Å)	18.663(5)	λ(Å)	0.71069
c(Å)	12.090(2)	R	0.037
β(deg)	99.39(2)	R_w	0.030
T(°C)	26		

Table 6-2. Selected Bond Lengths and Angles for $[Ag([18]aneO_2S_4)]^+$

Intramolecular Distances (Å)

atom	atom	distance	atom	atom	distance
Ag(1)	S(1)	2.594(2)	S(3)	C(7)	1.802(5)

Table 6-2. (continued)

Ag(1)	S(2)	2.603(2)	S(4)	C(8)	1.796(5)
Ag(1)	S(3)	2.585(1)	S(4)	C(9)	1.810(6)
Ag(1)	S(4)	2.593(2)	O(1)	C(4)	1.416(6)

Intramolecular Bond Angles (deg.)

atom	atom	atom	angle	atom	atom	atom	angle
S(1)	Ag(1)	S(2)	84.59(5)	Ag(1)	S(3)	C(7)	100.2(2)
S(1)	Ag(1)	S(3)	110.48(4)	S(1)	Ag(1)	S(4)	139.32(5)
Ag(1)	S(4)	C(8)	100.7(2)	S(2)	Ag(1)	S(3)	137.39(5)
S(2)	Ag(1)	S(4)	109.50(5)	S(3)	Ag(1)	S(4)	85.16(4)

Table 6-2.

The central silver(I) ion adopts a severely distorted tetrahedral geometry. It is surrounded by four sulfur atoms, and the two oxygen atoms do not interact with the metal ion. The S-Ag-S angles in the two five-membered chelate rings, as in the case of $[Cu([9]aneOS_2)_2]^+$, are compressed to 84.59(5)° and 85.16(4)° and the S-Ag-S angles in the two eight-membered metallacyclic rings are open to 137.39(5)° and 139.32(5)°.

The Ag-S bond lengths vary from 2.585(1) Å to 2.603(2) Å with an average distance of 2.594 Å, similar to those reported previously for $[Ag([9]aneS_3)Cl]$ [1] and $[Ag_3([9]aneS_3)_2]^{3+}$ [3] with

Table 6-3. Torsion Angles

Ligand Torsion Angles in [Ag([18]aneO_2S_4)]$^+$ (deg.)

atoms	angle	atoms	angle
S(3) C(6) C(5) O(1)	72.4(5)	S(3) C(7) C(8) S(4)	53.9(5)
S(4) C(9) C(10)O(2)	-57.0(5)	C(1) S(1) C(12)C(11)	-155.5(4)
S(1) C(1) C(2) S(2)	54.8(8)	C(1) C(2) S(2) C(3)	75.1(6)
S(1) C(12)C(11)O(2)	74.0(5)	C(2) S(2) C(3) C(4)	-96.1(5)
C(2) C(1) S(1) C(12)	72.4(6)	C(3) C(4) O(1) C(5)	-177.8(5)
C(4) O(1) C(5) C(6)	-161.9(4)	C(5) C(6) S(3) C(7)	-158.1(4)
C(6) S(3) C(7) C(8)	68.9(4)	C(7) C(8) S(4) C(9)	77.9(4)
S(2) C(3) C(4) O(1)	-56.6(6)	C(8) S(4) C(9) C(10)	-94.3(4)
C(9) C(10)O(2) C(11)	178.9(4)	C(10)O(2) C(11)C(12)	-164.0(5)

Torsion Angles for Free [18]aneO_2S_4 (deg.)

atoms	angle	atoms	angle
S(1) C(1) C(2) S(2)	174.5(1)	C(2) S(2) C(3) C(4)	71.0(2)
S(1) C(6) C(5) O(1)	178.6(1)	C(2) C(1) S(1) C(6)	69.3(2)
S(2) C(3) C(4) O(1)	-73.3(2)	C(3) C(4) O(1) C(5)	-174.0(2)
C(1) S(1) C(6) C(5)	174.5(1)	C(4) O(1) C(5) C(6)	-179.3(2)
C(1) C(2) S(2) C(3)	62.1(2)		

average length of 2.60 Å , but shorter than those in the octahedral species of $[Ag([18]aneS_6)]^+$ (average 2.742 Å) [2] and $[Ag([9]aneS_3)_2]^+$ (average 2.72 Å) [1].

Ligand torsion angles in $[Ag([18]aneO_2S_4)]^+$ are listed in Table 6-3, and for the sake of comparison, values for the free ligand are also presented. Significant change is found in two S-C-C-S linkages, which adopt anti placement (174.5°) in the free ligand, but turn to the unfavoured gauche orientation in $[Ag([18]aneO_2S_4)]$ (53.9(5)° and 54.8(8)°). These conformational rearrangements are apparently introduced by the coordination requirements. Interestingly, the two unfavoured anti C-S-C-C (174.5°) placements are still observed in the complex (155.5° and 158.1°), with only minor changes. This indicates, at least for $[18]aneO_2S_4$, that the ligand has a tendency to preserve its original conformation upon complexation, or in other words, even intrinsic conformation preference and complexation fail to perturb it significantly. This tendency ensures the minimal inversion enthalpy required to form metal complexes.

6.3. References

1. Blower, P.J.; Clarkson, J.A.; Rawle, S.C.; Hartman, J.R.; Wolf, R.E.; Yagbasan, R.; Bott, S.G.; Cooper, S.R., Inorg. Chem., *28*, 4040 (1989).
2. Blake, A.J.; Gould, R.O.; Holder, A.J.; Hyde, T.I.; Schröder, M., Polyhedron, *8*, 513 (1989).
3. Küppers, H.J.; Wieghardt, K., Tsay, Y.H.; Krüger, C.; Nüber, B. and Weiss, J., Angew. Chem Int. Ed. Engl., *26*, 575 (1987).